MCDA - Groundwater prediction analysis for Sustainable Development using GIS Supported AHP in Okeigbo, Southwestern Nigeria

Falowo Olumuyiwa[1], Philip Otuaga Moses[2]

1 Rufus Giwa Polytechinic, Owo
2 Federal University of Technology, Akure

Abstract

Multi-criteria decision analysis with GIS-supported Analytical Hierarchy Process (AHP) has been undertaken in Okeigbo, Southwestern Nigeria to predict the hydrogeologic significance of the aquifers and in relation to the geologic units; quartzite, quartz schist, and metadiorite. Six parameters of higher hydrogeologic importance were pairwise and weighted respectively: AQT - aquifer layer thickness (0.07), AQR - aquifer layer resistivity (0.16), OVT - overburden thickness (0.10), TR - transverse resistance (0.20), TMY - transmissivity (0.26), CoA - coefficient of anisotropy (0.22). Subsequently, the GWPIV ranged from metadiorite 1.08 (weathered/fracture aquifer) – quartz schist 3.55 (weathered aquifer) with an average of 2.35 indicating moderate groundwater potential. The low, moderate, and high zones constituted 25 %, 55 %, and 20 % respectively of the study area. The high potential zone is prominent in the mid-central and north central parts. Conclusively, the quartz schist and quartzite areas showed better prolificacy than metadioritic environment. But in terms of protective capacity of the aquifers, the longitudinal unit conductance recorded weak regional average of 0.19396 mhos, with quartzite (0.33444 mhos) and quartz schist (0.15218 mhos); and metadiorite recorded 0.1208 mhos, hence metadiorite being the weakest environment. The water table aquifer and the fracture basement are the major water bearing units in the area. The drainage basin falls within the low – moderate regional drainage basins, with moderate to high flow connectivity and low – moderate flow direction. Thus there's possibility of movement of water towards the northern part (discharged zone) with the southern area forming the watershed.

Olumuyiwa Olusola Falowo[1,*], Moses Philip Otuaga[2]

[1] *Department of Civil Engineering Technology, Rufus Giwa Polytechnic, Owo, Ondo State, Nigeria, ORCID:* http://orcid.org/0000-0003-3425-9072

[2] *Department of Applied Geology, Federal University of Technology, Akure, Ondo State, Nigeria, ORCID:* https://orcid.org/0009-0005-0270-5594

[*]e-mail: solageo@yahoo.co.uk

Introduction

Groundwater resource thorough assessment is important in ground water resource planning and management (Falowo and Daramola, 2023; Adagunodo et al., 2018; Bayewu et al., 2018; Tsepav et al., 2015; Falowo et al., 2020), even though It is also true that evaluating groundwater water supplies is difficult (Cosgrove and Loucks, 2015). The assessment of groundwater water sources across the nation poses additional challenges, especially in terms of data availability and maintaining consistency and similarity of results (Akanbi, 2017; Tartiyus et al., 2015). As a consequence, a trade-off between the best scientific techniques and their national applicability is crucial. Because ground water is a dynamic system, the assessment method must be regularly updated to keep up with technical advances, data access changes, and planning requirements (Mandel and Shiftan, 1981; ASCE, 1987; Harvill and Bell, 1986). Groundwater is a renewable but scarce resource, and forms an important part of the hydrologic cycle (Fetter, 2007). Groundwater resources in the aquifer are replenished and discharged on a regular basis by rainfall and other sources, resulting in variations in water level (Fetter, 2007; Todd, 1980). Below this zone of changing water levels, the aquifers remain constantly inundated. Excessive groundwater mining can diminish groundwater reserves, having serious social, economic, and environmental consequences. As a consequence, efforts have always been made to ascertain the usable quantity of groundwater resources, i.e. the volume of groundwater that can be extracted. Since it accounts for 97% of the earth's useable clean water supply, groundwater is an important resource for life and development. It can be found in voids, cracks, and permeable geological formations. Groundwater usage is ideal due to its accessibility, dependability, and widespread distribution. The global demand for pure water increases every twenty years. This elevated demand for groundwater clearly suggests that surface water will be insufficient to meet the expected overall demand. As a consequence, its rising demand is putting a huge burden on water sources. Many surface water sources have worsened or been depleted due to pollution, population development, deforestation in catchment areas, climate change, and over-exploitation, placing a burden on groundwater (Alley, 2004; Schwartz and Zhang, 2003; Bisson and Lehr, 2004; Falowo et al., 2017).

Aquifers are porous media with varying physical criteria and hydraulic conditions that greatly influence the quality of water they contain and are capable of supplying large amounts of water (Graham et al., 2006; Poehls and Smith, 2009). Groundwater quality typically changes horizontally and vertically, primarily due to aquifer boundaries or even from one geological structure to another within a single system. Furthermore, water salinity typically develops gradually within a flow media, even if it is a single bed, as a result of salts dissolution caused by groundwater movement between recharge and outflow zones, the groundwater capacity of each form of aquifer varies greatly from place to location or basin to basin (Gogoi, 2013; Walton, 1991; Wilson, 1983). The majority of the replenishment is accomplished through direct rainfall infiltration, while high intensity rains and cracks provide preferential replenishment. Okeigbo is a community in Ondo State, southern Nigeria, that has been experiencing severe pipe-borne water supply shortages for many years due to a variety of variables including geology, geomorphology, topography (recharge and outflow delineation), population growth, and so on.

Many citizens (over 500,000 people) rely on springs, which are not developed in many areas, streams, rainwater, rivers, and other bodies of water for household and civic purposes. Despite the fact that the government is required by the constitution to provide potable water to its citizens, as well as create, control, and operate groundwater systems, such duty is being transferred to community users, who cite a lack of funds as a significant impediment. Given that the community depends heavily on surface water, which is often contaminated by household, industrial, and neighbourhood discharges, as well as waste. Most of the wells created in the region have poor yields due to foundation rock interruption, which causes the wells to be abandoned. As a result, during the rainy season, atmospheric rainwater is the primary source of water for wells and waterways, as well as some springs.

Hence this calls for detailed groundwater exploration, in order to determine the extent of aquifer storage or nature and quality of the groundwater (Falowo and Daramola, 2023; Omer, 2018). Groundwater exploration has to do with all operations or activities that could lead to delineation of aquifer or underground reservoirs from which appreciable quantity and quality of water can be obtained with less operational cost. Hydrogeological studies usually involves geological analysis, collection of stratigraphic data, hydraulic properties determination, rainfall data analysis, geomorphology, and vegetation. The most critical aspect of groundwater investigation or hydrogeological exploration is the assessment of recharge either by direct method involving lysimeters or environmental or artificial tracers; or indirectly by determining the relationship between flow and the recharge (Amadi et al., 2017; Tizro et al., 2014; Halford et al., 2006; Johnson, 2005). Hydraulic characteristics of soil and hydrometeorology; landscape geomorphology; and geographic spread of hydro geologic units; and hydrography are all factors affecting groundwater recharge (Raghunath, 1987).

Furthermore, hydrogeological exploration provides knowledge on water-rock interaction, allowing for a better grasp of the aquifer's development. Groundwater research provides for the assessment of inherent vulnerability using various techniques. Knowledge of the population's anthropogenic activities serves as the foundation for estimating the prospective or real pollution burden that could endanger the quality of water in an aquifer. The risk of groundwater contamination is deduced from the relationship between intrinsic vulnerability and pollution load (Bayewu et al., 2018 Aina et al., 2019; Opeyemi et al., 2016; Mazac et al., 1985). Geophysical methods, hydrogeological measurements, remote sensing techniques, and geological investigations are frequently used in groundwater investigation, while DRASTIC, GOD, and Aquifer Vulnerability Index (AVI) are commonly used for pollution/contamination evaluation. Geophysical methods such as electrical resistivity, seismic, very low frequency electromagnetic, borehole logging, and magnetic methods are commonly used to identify the volume and structure of the groundwater, as well as its geometry and structural elements (Sajeena et al., 2014; Abdullahi et al., 2015; Tweed et al., 2007; Minaibim et al., 2022).

In contrast to borehole recording, electrical resistivity is the most flexible of all non-destructive geophysical techniques used in groundwater research because it is very dependable, fast, and cost effective in finding and describing aquifer geometry (Abdullahi et al., 2015; Bawallah et al., 2019; Chaanda and Alaminiokuma, 2020). The hydrogeological data (from the pumping test) aids in determining the hydraulic conductivity, transmissivity, and specific yield of the groundwater reservoir. Permeability and porosity are two of the main characteristics that govern the storing and flow of water in an aquifer, and their significance in groundwater or hydrogeological issues cannot be overstated (Gao et al., 2018). Despite the existence of simple models and correlations relating resistivity and aquifer hydrologic characteristics, pumping is still regarded as the

most qualitative approach in determining these properties such as transmissivity, specific yield, hydraulic conductivity, specific capacity, and storage coefficient (Delleur, 1999; Kruseman and de Ridder, 1991; Nwosu et al., 2013; Bear, 1979; Driscoll, 1986). In addition, remote sensing technique will aid in the geological recording of fracture zones prone to groundwater accumulation (Tweed et al., 2007; Meijerink, 2007; Shaban et al., 2006). The study's goal was to evaluate the potential of groundwater resources and their susceptibility to pollution. The study will define the principal hydrogeologic units and their distribution, recharge and discharge areas, and general groundwater potential zonation. The method utilized integrated survey methods so as to develop a prediction model of high validity and reliability for proper management of the resource.

Material and Method

Description of the Study Area

The study area is Okeigbo, which is located between 689000 m and 694000 m East and 790000 m and 794500 m North of southwestern Nigeria (Figure 1) in Ile Oluji/Okeigbo Local Government Area of Ondo State, Nigeria. It shares boundaries in the East with Ondo town and Ifedore Local Government Areas of Ondo State and in the west by Osun State. The town is a built up area (Figure 2) surrounded by rocks from which it derived its name from, Oke (hills) and Igbo (forest). The climate is of tropical rain forest characterized by wet (April to September) and dry season (October to March).
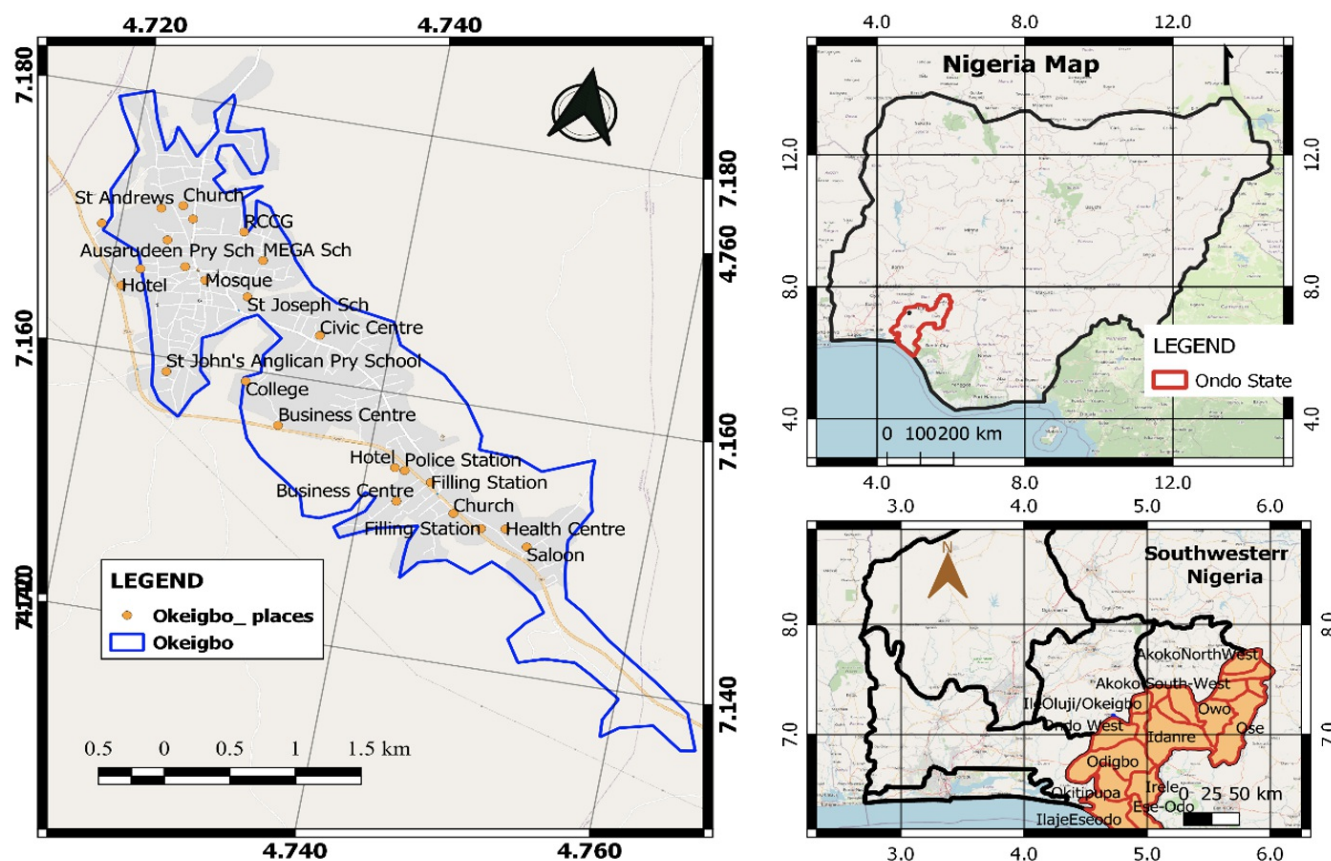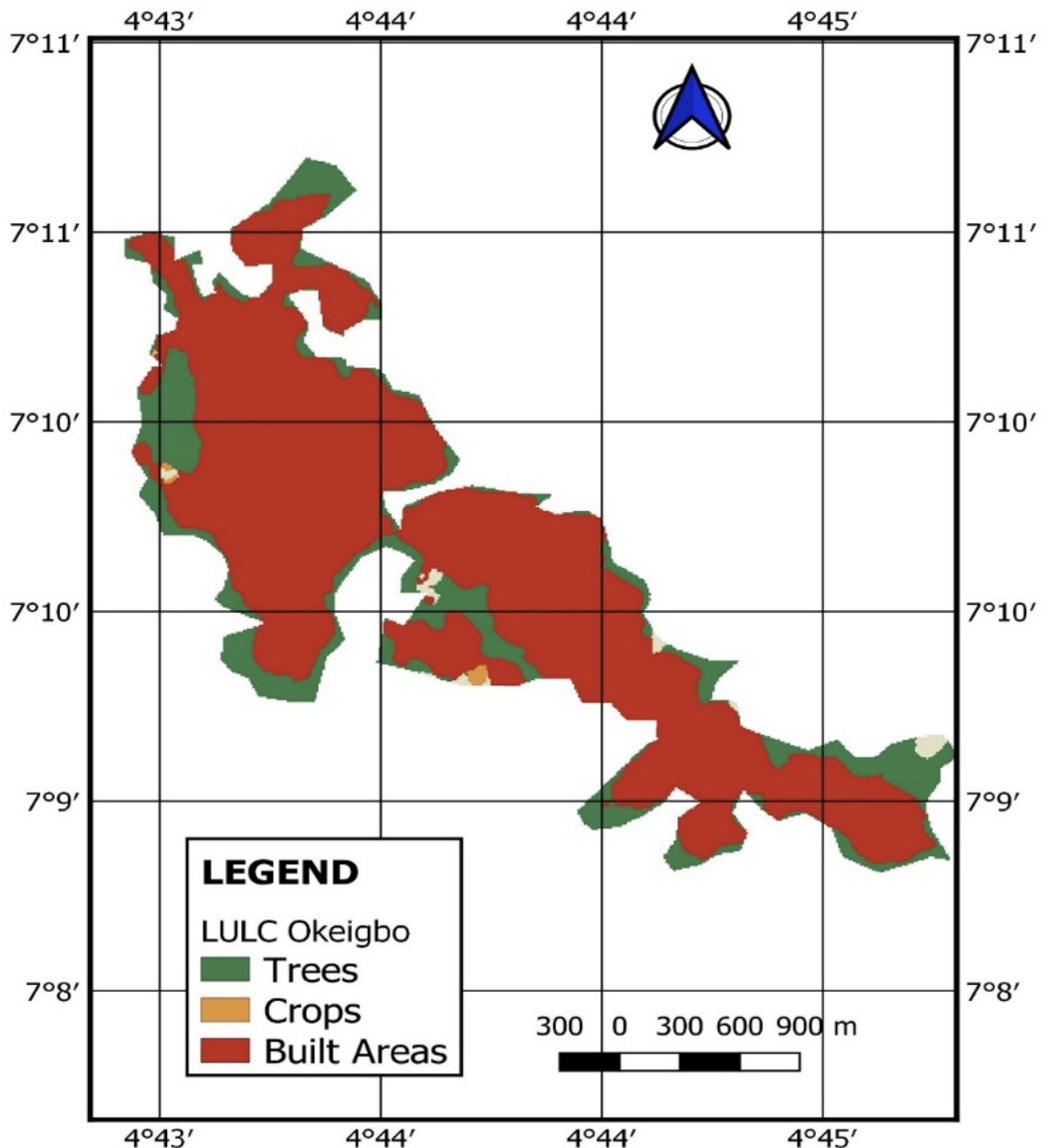

Figure 1. Location map of the Study Area on the map of Ondo State, Southwestern Nigeria

Figure 1. Location map of the Study Area on the map of Ondo State, Southwestern Nigeria

Figure 2. The land use/land cover map of Okeigbo Metropolis, which is predominantly built up area (modified after Living Atlas, 2010)

The mean annual rainfall is 1500 mm, the average temperature (at peak) is 32°C especially in February and 25°C in August (Iloeje, 1981). The relative humility is 70% in January to 90% in July; while the elevation varies between 190 – 270 m (Figure 2a). The drainage pattern in the area is dendritic while groundwater is primarily recharged by precipitation and

secondarily by lateral flow from rivers and their tributaries. The geology of the area is that of the basement complex of southwestern Nigeria (Figure 3), with four main lithological groups, migmatite-gneiss-quartzite complex, schist belts, Older granites, and minor intrusives. However lithologic units observed in the area are quartzite which is flaggy, quartz metadiorite, and quartz schist (Figure 4). Many of the places underlying by schist and quartzite is generally concealed by a variable thick overburden which in many places are clay or laterite. In many places, the quartzite are found in association with quartz schist, and are concealed by a variable thick overburden which in many places are clayey or laterite. The observed Quartzite occurred as boulders, elongated ridges and weathered rock; has fine texture and non-foliated, formed by both contact and dynamic metamorphism or from cementation of silica, with the principal mineral being quartz. The colour of the quartzite varied across the study as white, pink, yellow or gray tints, depending on its impurities. The observed mineralogy consists of quartz, with zircon, hematite, tourmaline, muscovite, staurolite, graphite, sillimanite as minor minerals (Obaje, 2009). Structural feature such as joints and fractures were observed, and in many places are filled with laterite or clayey sand. The Schist on the other hand are megascopically crystalline foliated metamorphic rocks characterized by a typical schistose structure. The constituent flaky and platy minerals are mostly arranged as parallel or sub parallel layers or bands. They are characterized by textures with marked preferred orientation.
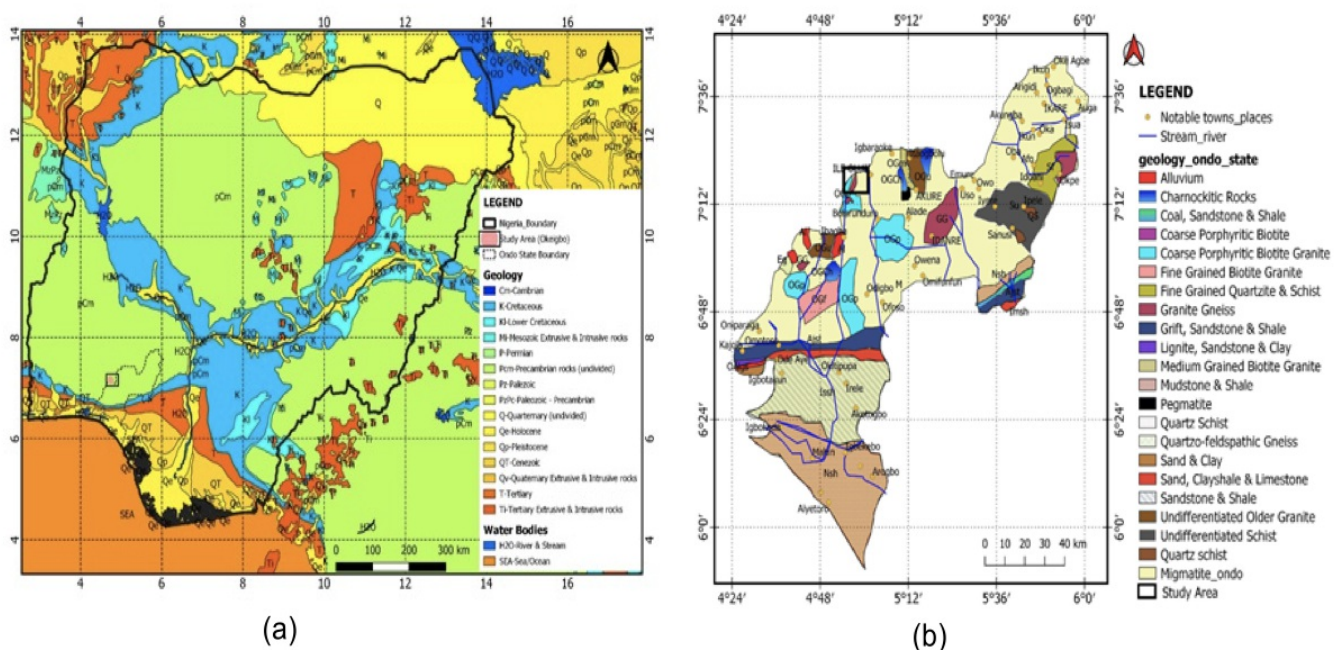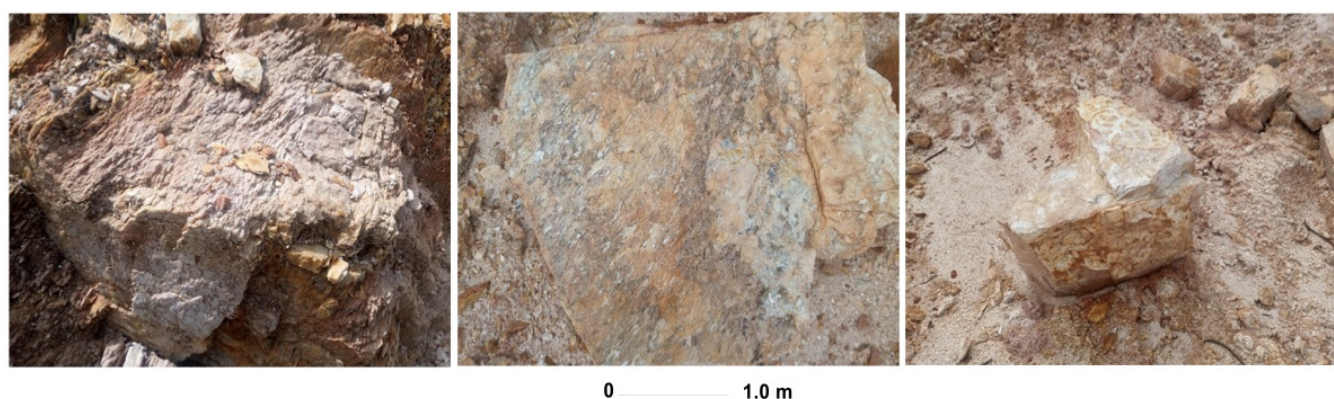

Figure 3. Geological map of (a) Nigeria and (b) Ondo State showing the study area, which falls within the Southwestern Basement Complex Nigeria with migmatite being the predominant rock unit (modified after NGSA, 2006)
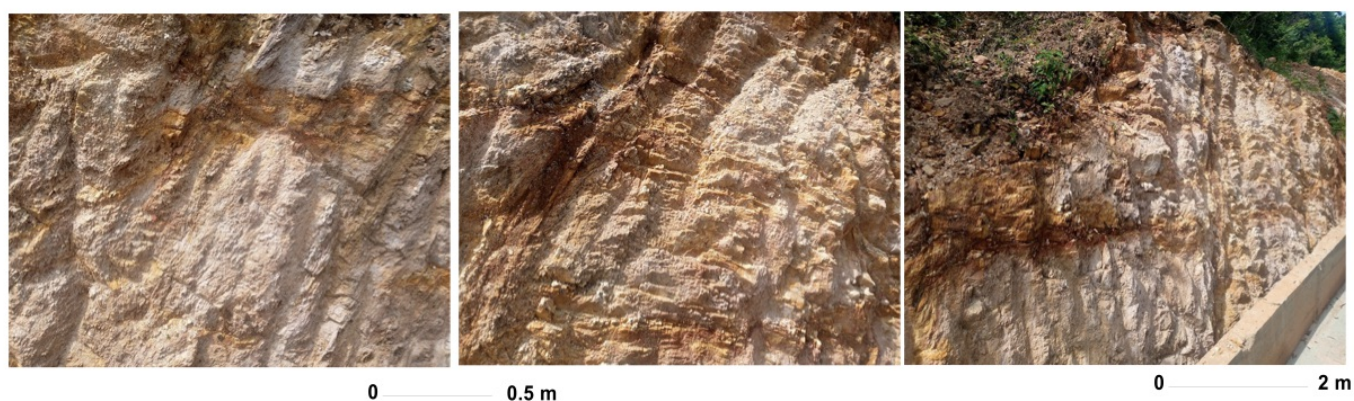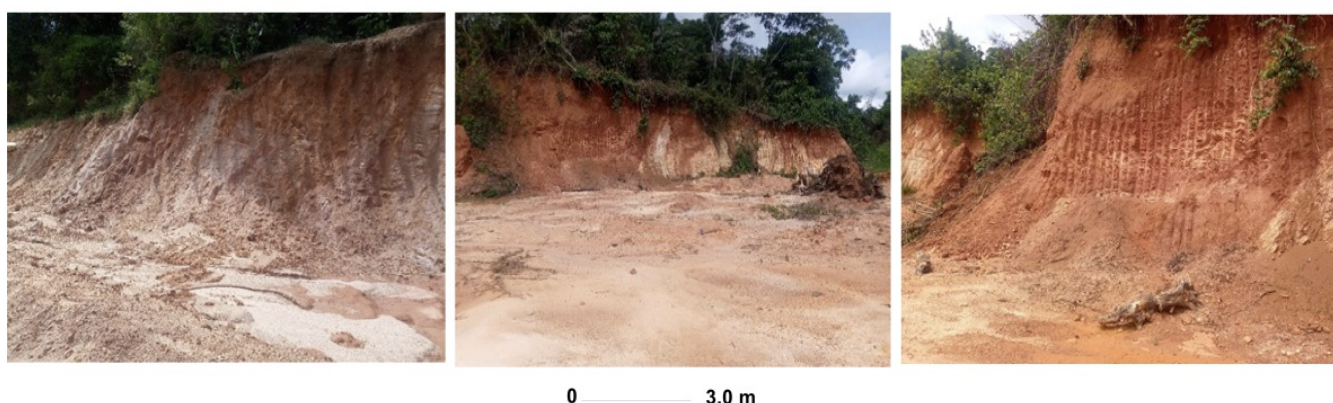
- Mica/quartz Schist exposed at different locations by road-cut with forms of mineral orientaion (slaty cleavage)

- Highly weathered flaggy quartzite

- Exposure of thick deposit of weathered products (laterite and clay) of Schists and quartzite in the study area

Figure 4. Major Geological units observed in the Study Area ranging from quartzite, and quartz schist

These preferred alignment of platy minerals accounts for their schistocity. They appear appreciably stronger across than along the mineral lineation. It is medium to coarse in texture, and foliated with schistose structure. It contains readily visible slaty cleavages. Mica and chlorite are common minerals, with feldspar in lesser amounts; quartz and feldspar are comparatively rare or minute (Obaje, 2009). In the area, the Quartz schist been affected by intense weathering, as they split along the plane of weakness. In the Schistose quartzite, the less resistant minerals have been eroded leaving the more resistant minerals such as quartz and feldspar. Not only those cleavage and schistocity adversely affect the strength of schist, it also makes them susceptible to decay. In fact schist weather slowly but could undergo extensive regional

metamorphism resulting in folding, fracture. Weathered material (formed by weathering activities) and fractured basement aquifers (formed by tectonic/orogenic activities) are the hydrogeologic units in the area. The greatest groundwater potential zones are those in which the fractured foundation rests beneath the weathered zone. The overburden in most cellar topography is typically thin, making it susceptible to vertical source movement pollution via infiltration, leaching, and inundation. Joints, faults, folds, foliations, intrusions, and rock-to-rock interactions are examples of structural characteristics found on lithologic units. The structural characteristics run in the NNW-SSE and NNE-SSW directions. Springs (about seven) from the hills, rivers, and streams were noted in the region as the community's supply of water.

This soil material (Figure 4) consists of a thick deposit of laterite and sandy clay (which forms part of lithosols as shown in Figure 5) at various locations throughout the study area, weathered rock material, some of which occurs as boulders are excavated and transported to construction sites for various projects such as highway construction, embankment, and fillings. Lithosols are a form of azonal soil that consists primarily of unweathered or partially weathered rock pieces and is typically found on steep hillsides or in groups of shallow soils with poorly defined horizons. Azonal is a soil major group that is frequently categorized as the highest rank, encompassing soils that lack well-developed horizons due to immaturity or other factors that have hindered their growth.

Data Acquisition and Analysis

The terrain is rocky and rugged, therefore it makes drilling difficult at a very low cost. This singular phenomenon usually scares many drillers, which may not compensated by many clients. This terrain characteristic is not strange, as the case in the basement complex, where prolific aquifer is a function of nature of weathered rock material and availability of secondary porosity or fracture zone in the rock (Hiscock, 2005). The local rainfall is the major recharge for the aquifer system in the area. Furthermore, the extreme variation in lithology and high localization of geologic structures make geological, and hydrogeological exploration for groundwater difficult. Therefore the geoelectric parameters that would be of hydrologic significance will be largely determined by the prevailing factors that influence the occurrence of the resource in the area. The data acquisition map is shown in Figure 6.
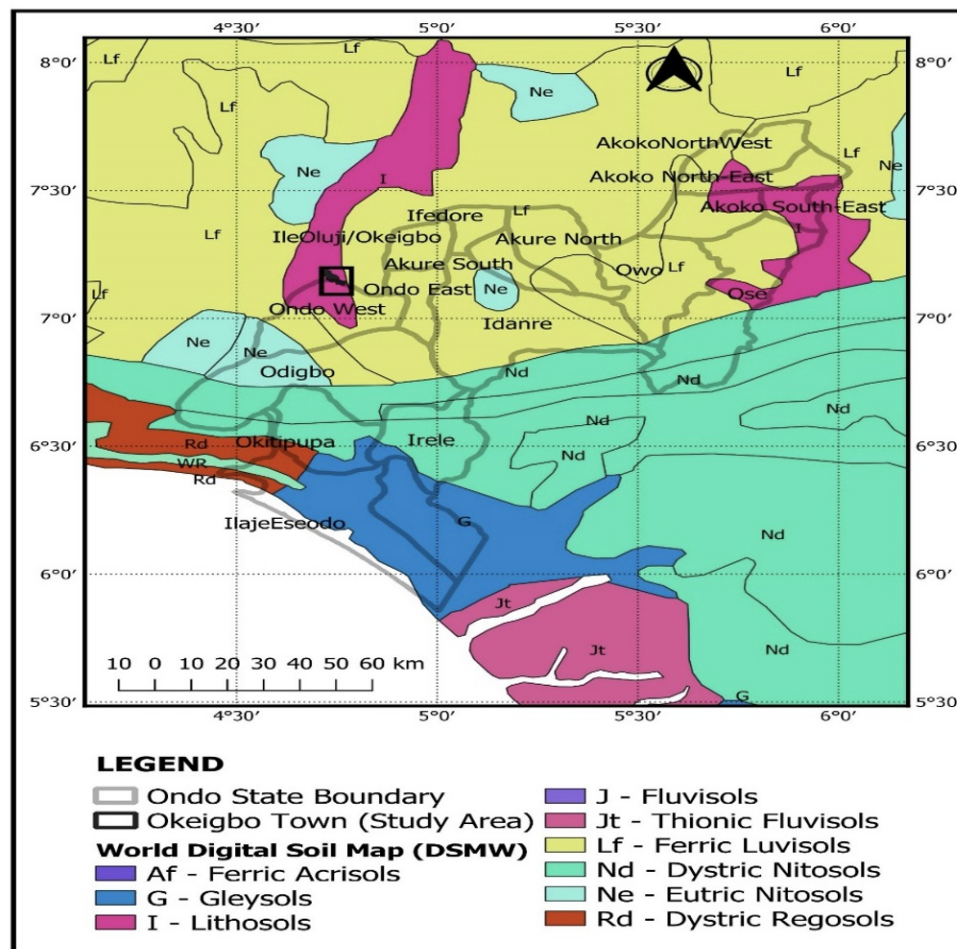
Figure 5. Soil map of Nigeria, with the study area falling on Lithosols (modified after FAO/DSMW, 2020)

Hydrogeological prospecting entails the creation of hydrogeological maps, the chemical analysis of water wells and boreholes, the observation of the water table, the delineation of groundwater bodies, and the determination of their type based on pumping test (by determining the rate flow, draw down, and radius of influence). The direct and indirect methods were used for this study because groundwater occurrence and movement are primarily controlled by the aquifer's permeability and the lithology of the underlying strata (Olasehinde et al., 2015). The direct method involved measuring hydraulic parameters from boreholes/open wells and by pumping tests; mapping outcrops and geomorphology of the area; and the indirect method involved geoelectric sounding using vertical electrical sounding (VES). However, before embarking on the field survey, the drainage basins, river network, or watersheds were studied using a geographic information system; a review of available information on hydro census of boreholes in the area; geological formation in terms of lithology and structures; hydrogeological information regarding aquifer system, and groundwater occurrence were assessed. Climate, vegetation, drainage, and soil material were all examined as well.

The digital elevation model (DEM), hill shade, slope, and aspect (direction of slope) was produced using Quantum Geographic information system (QGIS) software. The elevation raster data/shape file was acquired from USGS website (https://earthexplorer-USGS) using SRTM 1 Arc Second Elevation file, and launched in QGIS and modified using SAGA tool. The drainage channel, stream network or catchment area, basin analysis were done using the processed DEM and the

DEM was filled using the Wang & Liu tool under terrain analysis hydrology. The stream network was created using Shrahler order in SAGA analysis tool. The land use/land cover was done by downloading the ESRI shape file from "living atlas of the world" website, and launch in QGIS, where it was processed and clipped to the study area.
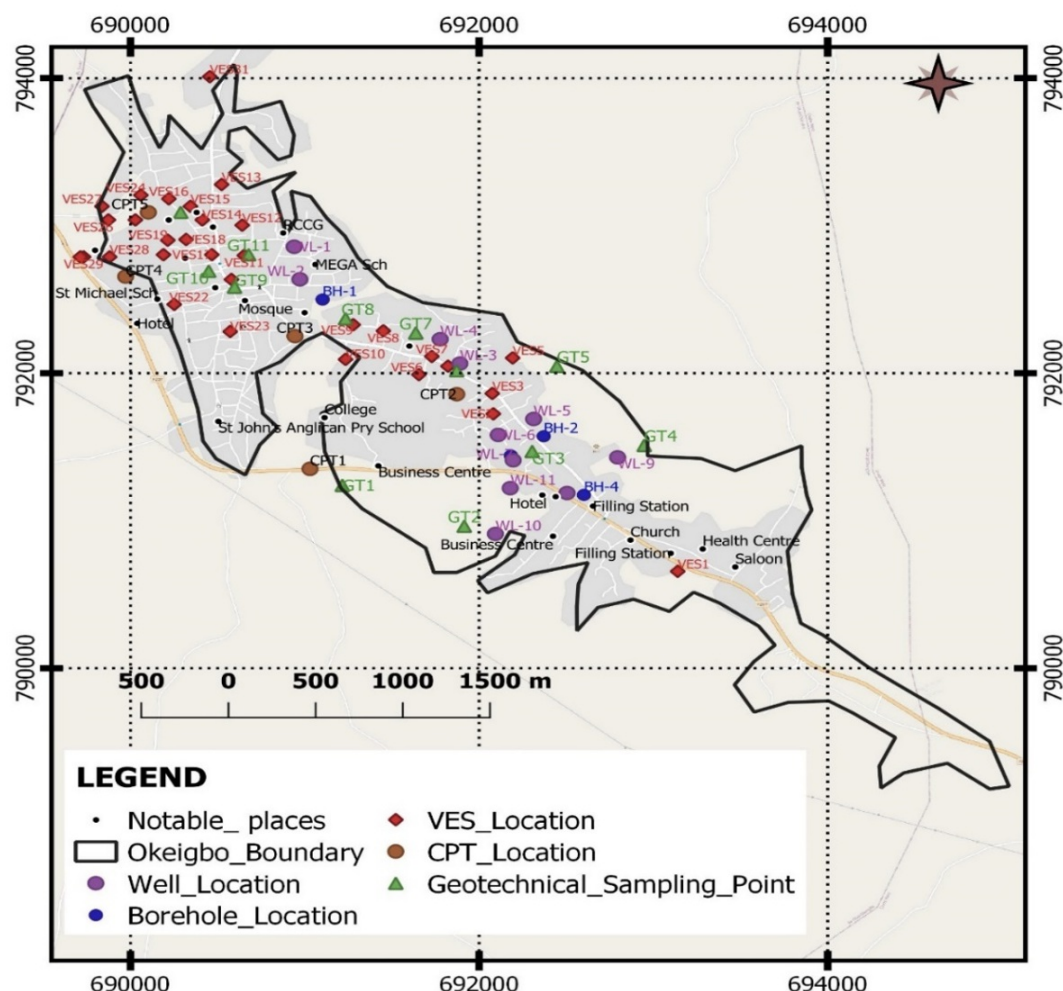
Figure 6. Data acquisition map for the study showing different locations where data were collected from the wells, VESs, and boreholes

Geological investigations included traditional mapping of rock groups and structural element assessment on outcropping portions using a compass clinometer. GPS was used to capture position data of rock kinds and geological formations such as fractures and faults, as well as locally accessible information such as altitudes and surface water body locations. These data were used to help interpret information from satellite images. Aquifer testing was performed to determine the hydraulic parameters of the aquifer, including transmissivity, hydraulic conductivity, and aquifer yield (Kruseman and de Ridder, 1991; Nwosu et al., 2013; Anomohanran, 2013). Pumping tests entail continuously pumping water from a test well and monitoring the water level over time. This drop in water level causes the water around the well to flow toward the well. The difference between the measured depth and the static water level gives the drawdown values used in estimating transmissivity and storativity. Pumping was carried out with a 0.5 horse power pump at each location using normal aquifer pumping test and single well testing. As water was pumped from the test well, the water level in the observation well located between 15 - 50

m from the test well was monitored for a specific interval. The transmissivity and storativity of the aquifer were determined by the Jacob straight-line method. A graph of draw-down (h_0– h) was plotted on an arithmetic scale against time plotted in logarithmic scale.

The drawdown per log cycle was determined from the graph and was used to compute the transmissivity (T) and storativity (S) of the subsurface aquifer (equations 1-2). The duration of the pumping was determined by the type of aquifer and the degree of accuracy desired in establishing the hydraulic characteristics. The obtained drawdowns were compared with the thickness of the wells' thicknesses, and were all less than 5% of the aquifer thickness (Kruseman and de Ridder, 1991; Logan, 1964). Consequently no correction was made on the obtained drawdown values.

$$T = \frac{\frac{2.3Q}{4\pi\Delta S}}{} \quad (1)$$

$$S = \frac{\frac{2.25Tt_o}{r^2}}{} \quad (2)$$

Furthermore, information on existing open wells (11) and boreholes (04) was obtained, and measurements of static water level, hydraulic head, total depth, thickness of water columns, and other parameters were obtained using a geographic positioning system and steel tape with the lower end marked to allow readings from the submerged portion. Two readings were taken at each well/borehole location to ensure precision, and the average values were computed whenever there was a discrepancy. Because the depth to the static water level is considered an indication of the interface between the vadose and phreatic zones in a non-confined aquifer setting (Brassington, 1988), the measurements were used to determine the thickness of the vadose zone across the area Borehole recording was also used to assess the nature and thickness of the various geological elements entered by wells and test shafts. The four boreholes were drilled using rotary percussion to determine the underlying topography and makeup of the reservoir. To ensure high-quality, long-term groundwater, aquifer characteristics established by borehole recording and flow testing must be integrated (Akanji and Olorunfemi, 2021).

The VES resistivity survey was carried out using Ohmega meter. Thirty one VES points were positioned in the study area using Schlumberger electrode configuration with half-current electrode separation (AB/2) ranging from 1 m to 150 m. The apparent resistivity values were obtained as the product of the resistance read from the resistivity meter and its corresponding geometric factor (K) for each electrode separation. The apparent resistivity data were then plotted against AB/2 on a bi-logarithm graph as sounding curves. The plotted sounding curves were interpreted manually by partial curve matching using different master curves. The geoelectric parameters from the partial curve matching served as the input model for computer-assisted iteration using WIN resist software. The values of the longitudinal unit conductance (LC), reflection coefficient (RC), fracture contrast (FC), transverse resistance (TR), formation factor (FM) and coefficient of anisotropy (CoA) serve as the basis for the characterization of its aquifer potentiality and protective capacity. The longitudinal unit conductance gives a measure of the impermeability of the confining clay layer, which has low resistivity and low hydraulic conductivity. The protective capacity of the overburden layers in a particular area is proportional to the longitudinal unit conductance. The longitudinal layer conductance (S) of the overburden at each VES station was obtained as shown in equation 4.

$$LC = \sum_{i}^{n} \frac{h_i}{\rho_i} \quad (4)$$

The reflection coefficient was determined using equation 5.

$$Rc = \frac{\left(\rho_n - \rho\right)(n-1)}{\rho_n + \rho(n-1)} \quad (5)$$

Where r is reflection coefficient, ρ_h is the layer resistivity of the nth layer and $\rho_{(n-1)}$ is the layer resistivity overlying the nth layer. The fracture contrast was calculated using equation 6.

$$F_c = \frac{\rho_n}{\rho_n - 1} \quad (6)$$

The traverse resistance was calculated using equation 7:

$$T = \sum_{i=1}^{n} \rho_i h_i \quad (7)$$

where T is traverse resistance, ρ and h are resistivity and thickness of the nth layer respectively. Using the geoelectrical parameters. The longitudinal resistivity (ρ_l), transverse resistivity (ρ_t), and coefficient of anisotropy (λ) are used in assessing overall aquifer potentiality (Utom et al., 2012) using geoelectrical parameters of resistivity and thickness, hence equations 8 – 10 were used.

$$\rho_l = \sum_{i}^{n} \frac{h_i}{S_i} \quad (8)$$

$$\rho_t = \sum_{i}^{n} \frac{T_i}{h_i} \quad (9)$$

$$\lambda = \sqrt{\frac{\rho_t}{\rho_l}} \quad (10)$$

The F_M combines all properties of the material influencing electrical current flow like digenetic cementation, pore shape, and porosity. In this study, the obtained F_M was correlated (r^2) with hydraulic conductivity. The formation factor was derived using equation 11. The conductivity (in mhos) of water at site was measured first using conductivity meter and converted to ohm-m. The average F_M calculated for each of this geological units was used to determine the hydraulic conductivity of aquifers with no well/borehole data.

$$F_M = \frac{\text{average aquifer water resistivity}}{\text{resistivity of water at site}} \quad (11)$$

Results and Discussion

Terrain Analysis, Drainage Network, and Basin

Figure 7 showed the processed DEM, hill shade, slope and aspect maps obtained for the study area. The DEM map showed variation of 197 – 320 m above the sea level. The higher elevations are generally remarkable in the southern area (216 - 236 m), while the lower elevations characterized the northern part. This implies that there possibility of movement of water towards the northern part (discharged zone) with the southern forming the watershed. Watershed is defined as the region draining into a stream, stream system, or body of water. A watershed map reads the data from a grid file and splits the grid up into basin, or catchment, areas. In addition, the hill shade showed varying forms of altitude: low land (designated as 1) and higher lands (>61), however the range of 1 – 61 % is the most dominant; which infers that the altitude of the rock units or landforms varies from low – moderate but sloppy above 70 %. The aspect which is the direction of the slope showed prevailing values ranging from 143 to >287 in the southern part, while 1 – 43 degrees in the northern area.

The drainage network and catchment area is shown in Figure 8. The area is well drained by many river channels. Basin areas are areas that drain water to the stream. The channels shown in Figure 6 are the major rivers in the study with shrahler order (in QGIS) greater than 5, which means that the minor streams have been cut off from the map during processing. An attempt was made to know the major catchment channel(s) or boundary supplying two watershed points at the northern part, the maps revealed that all the channels serve as contributors to those points as they are generally interconnected, hence the catchment area for the area is large. Figure 9 represents the drainage basin of the study area, and falls within the moderately low regional drainage basins. The flow direction and connectivity (Figure 10) of the surface water in the study showed moderately high direction flow, however the flow direction of the streams/rivers are generally lower and higher in northern and southern parts respectively (Figure 10a). But flow connectivity ranged from low (0) to moderate (3) (Figure 10b).
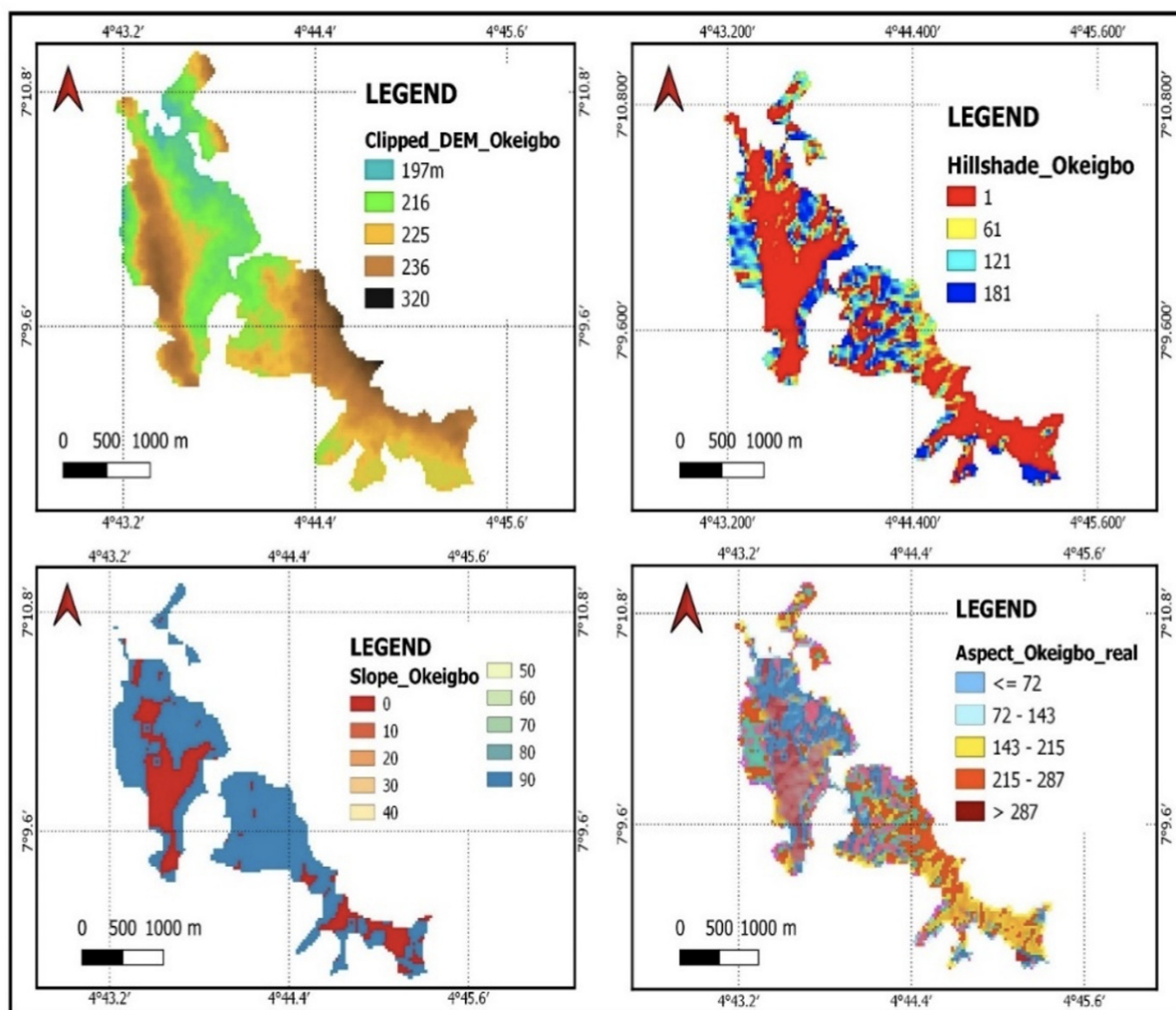
Figure 7. Maps of the digital elevation model (DEM), hill shade, slope, and aspect developed from Quantum geographic information system for the study area
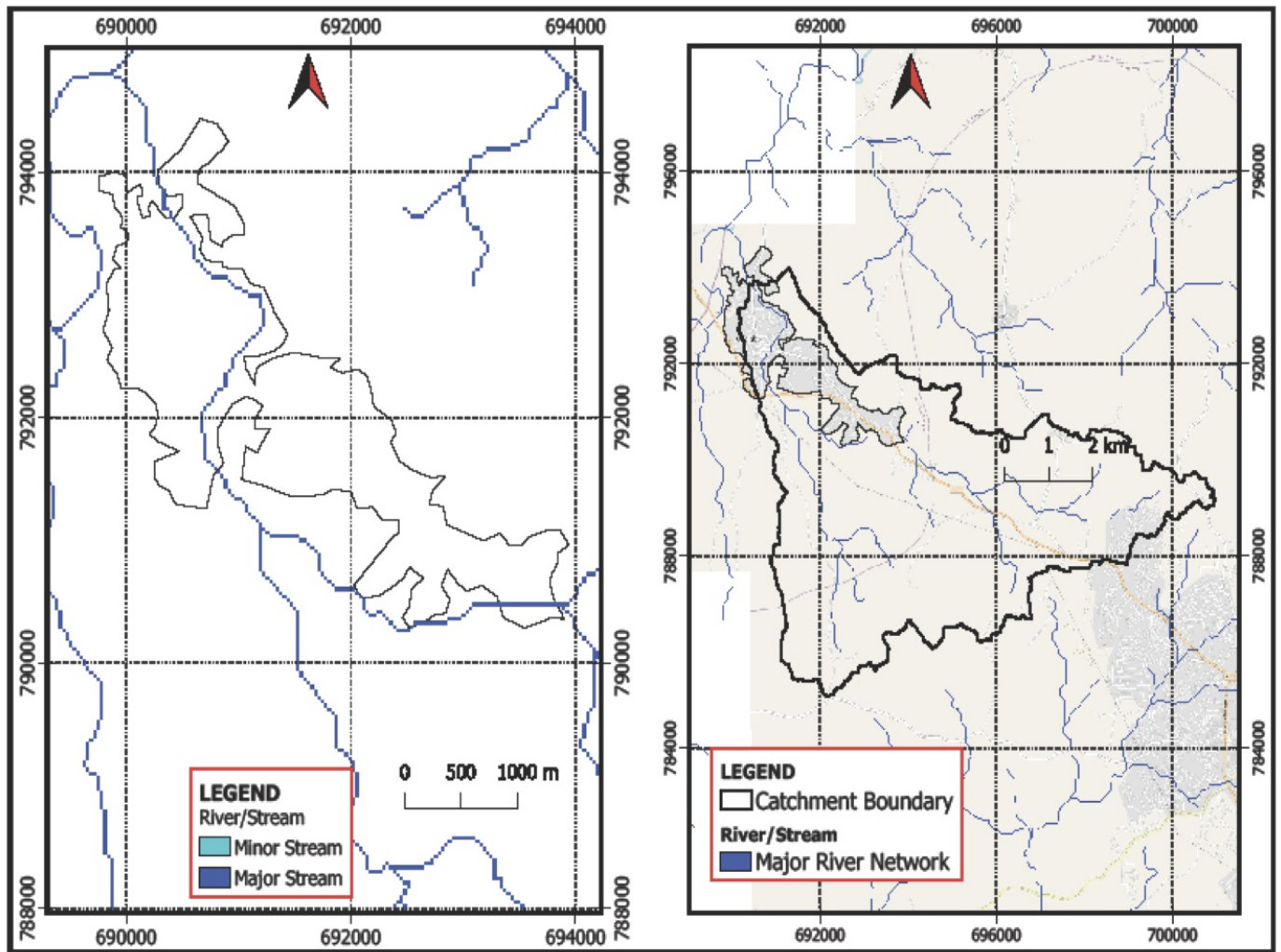
Figure 8. Maps showing the (a) drainage network (b) catchment boundaries for two catchment points at the northern and southern parts.
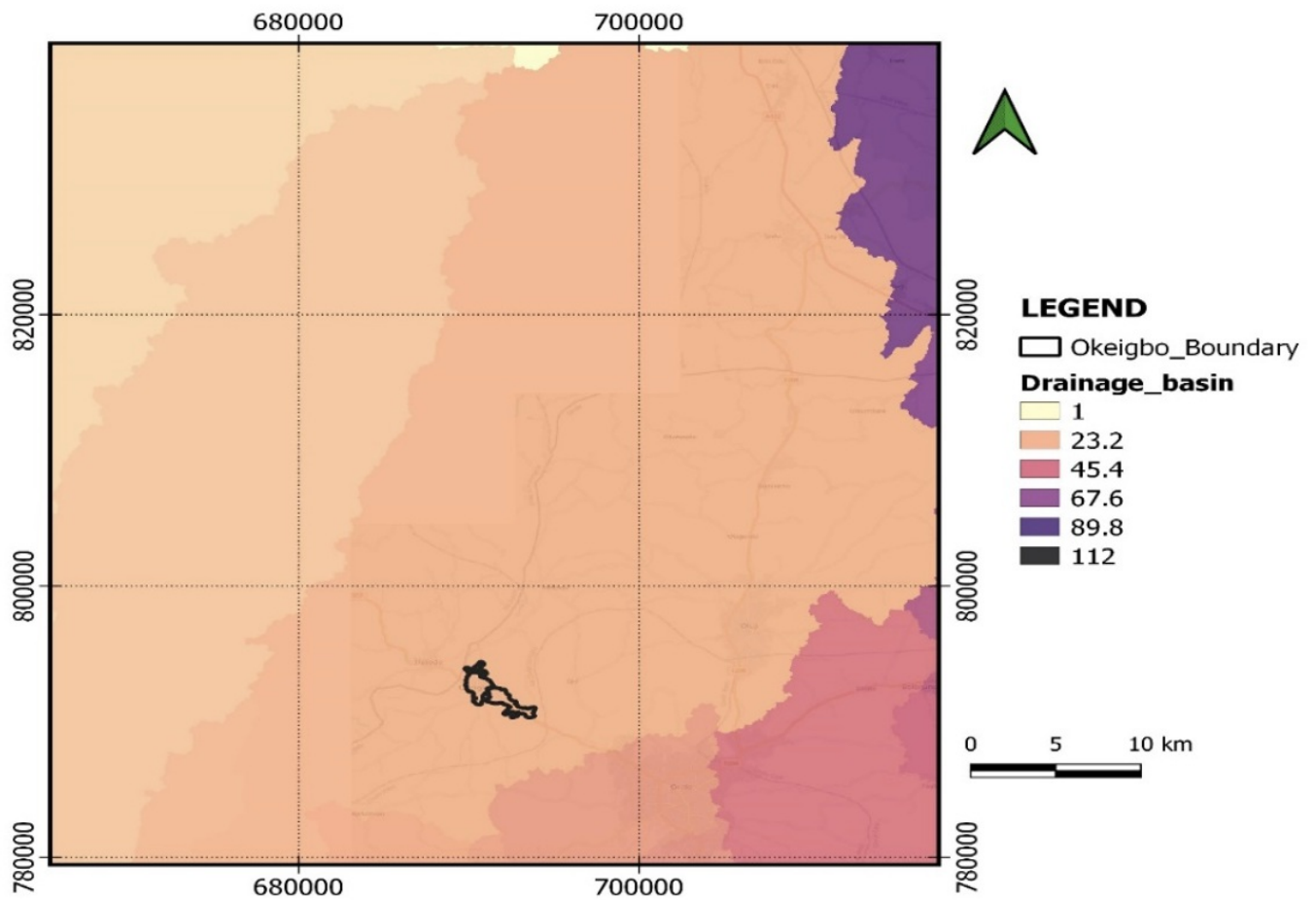
Figure 9. Maps showing the study area's drainage basin type
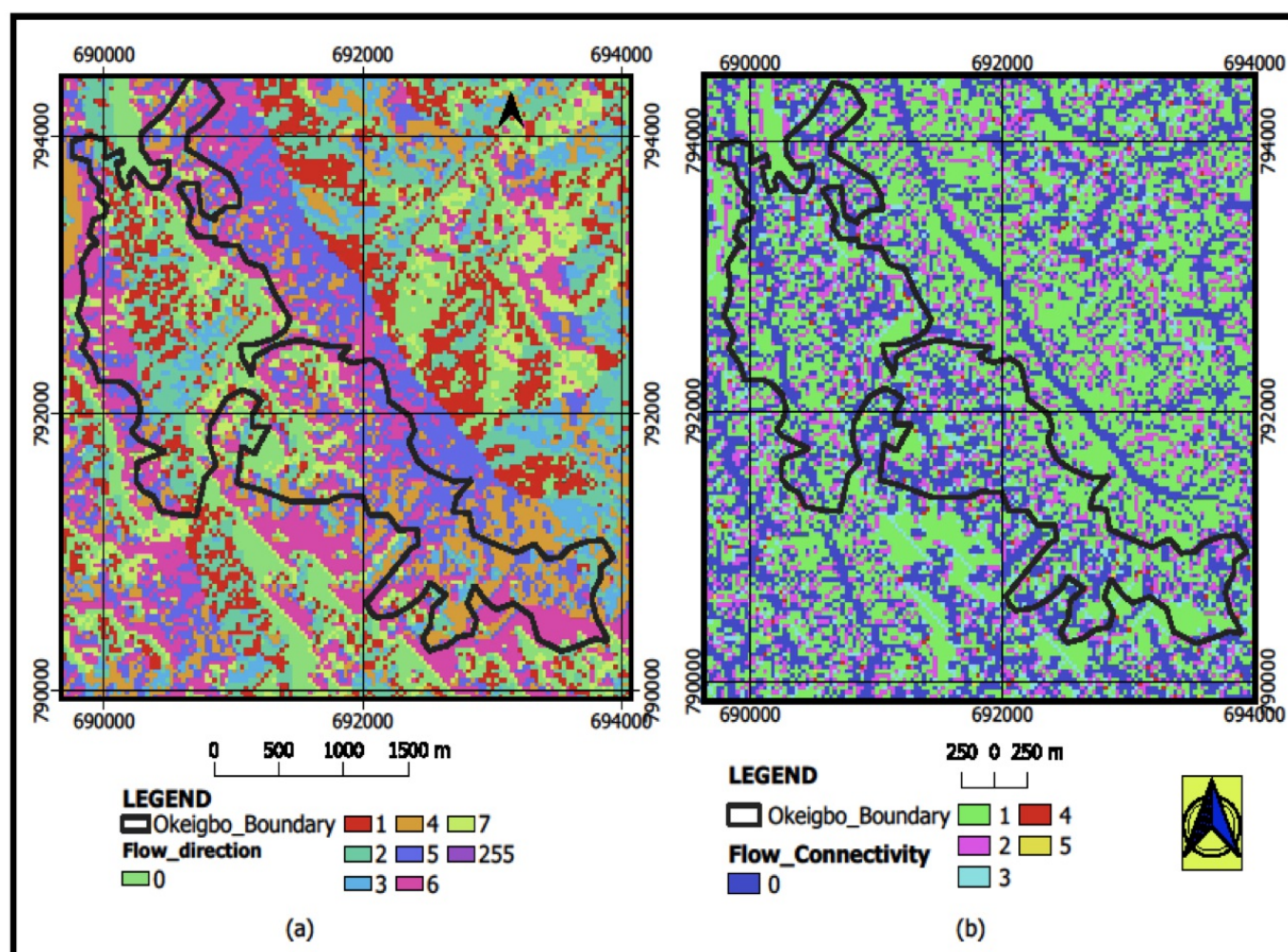
Figure 10. Maps showing the study area's (a) degree of its flow connectivity (b) flow direction

Geoelectric Characteristics and hydrogeologic units Delineation

The summary of the VES is presented in Table 1, while a typical geologic section prepared for VESs 2, 6, 10, 22, 23, and 28, in SE – NW trend, is shown in Figure 11. The H curve type is the most preponderant (34 %) followed by KH (24 %), HKH (22 %), QH (14 %), and KHKH (6 %). %). It is often possible to make qualitative hydrogeologic deductions from curve types. This implies that the area is generally made of high resistive topsoil, underlain by high conductive weathered layer, and basement rock. The VES interpretation, summarized in the table inserts, revealed three to five geoelecric layers, consisting of topsoil, subsoil, weathered layer, partly weathered/fractured basement, and fresh basement. This implies that the area is generally made of high resistive topsoil, underlain by high conductive weathered layer, and basement rock. From Table 1, topsoil has resistivity ranging from 36 – 2363 ohm-m (avg. 255 ohm-m) and thickness varying from 0.7 – 4.9 m (avg. 1.55 m) and composed of clay, sandy clay, clayey sand, sand, and laterite. The subsoil is characterized with resistivity ranging from 96 – 3561 ohm-m (avg. 1149 ohm-m) and have same composition as the topsoil, with thickness ranging from 1.5 to 15.8 m (avg. 5.68 m).

Table 1. VES Interpretation Results for the Study Area

| East	North	Elevation (m)	VES NO.	Resistivity (Ohmns-meter)					Thickness (m)				Depth (m)				Curve Type
				ρ_1	ρ_2	ρ_3	ρ_4	ρ_5	h_1	h_2	h_3	h_4	d_1	d_2	d_3	d_4	
693140	790657	228	1	188	312	1332			1.9	14.2			1.9	16.1			H
692082	791725	247	2	222	96	854	258		0.8	3.2	4.2		0.8	4	8.2		HK
692076	791863	245	3	55	290	102	2111		1.8	1.5	10.2		1.8	3.3	13.5		KH
691822	792048	231	4	350	185	1875	226	3255	1.1	2.9	8.3	13.9	1.1	4	12.3	26.2	HKH
692193	792104	241	5	186	843	302	2259		1.1	3.6	19.7		1.1	4.7	24.4		KH
691655	791991	227	6	159	374	86	668		1.9	2.4	8.9		1.9	4.3	13.2		KH
691729	792114	227	7	303	999	55	1113		2.3	9.6	12.3		2.3	11.9	24.2		KH
691451	792288	218	8	405	991	112	2531		0.9	8.6	17.8		0.9	9.5	27.3		KH
691278	792329	212	9	224	2587	47	1236		1.6	3.8	15.3		1.6	5.4	20.7		KH
691234	792094	213	10	2363	1212	66	2303		2.5	8.7	16.3		2.5	11.2	27.5		QH
690653	792799	224	11	195	2637	126	3303		4.6	3.9	12.2		4.6	8.5	20.7		KH
690641	793004	220	12	147	3561	144	3362		4.9	3.8	19.9		4.9	8.7	28.6		KH
690523	793280	217	13	151	1005	38	3652		1.2	7.9	8.2		1.2	9.1	17.3		KH
690412	793040	234	14	158	1488	265	2105		1.9	7.4	9.7		1.9	9.3	19		KH
690344	793132	237	15	89	1145	69	3647		1.1	6.7	14.1		1.1	7.8	21.9		KH
690220	793183	240	16	155	1063	88	899		1.2	3.9	19.3		1.2	5.1	24.4		KH
690467	792804	235	17	78	277	95	2212		1.1	9.3	13.4		1.1	10.4	23.8		KH
690319	792907	243	18	389	784	111	2197		0.9	1.5	25.5		0.9	2.4	27.9		KH
690214	792902	243	19	80	1176	78	4520		1.6	8.8	19.8		1.6	10.4	30.2		KH
690189	792804	247	20	408	878	123	2998		0.8	15.3	15.4		0.8	16.1	31.5		KH
690579	792636	235	21	83	654	101	1222		0.7	2.4	9.9		0.7	3.1	13		KH
690251	792467	265	22	55	325	85	665		0.8	7.4	20.5		0.8	8.2	28.7		KH
690572	792283	244	23	265	989	94	3017		1.2	2.9	18.4		1.2	4.1	22.5		KH
690059	793208	230	24	175	1202	323			1.9	12.3			1.9	14.2			K
690028	793040	224	25	37	1032	258	2141		0.9	3.4	9.9		0.9	4.3	14.2		KH
689873	793040	200	26	187	3117	285	888		1.9	2.2	14.8		1.9	4.1	18.9		KH
689836	793132	197	27	225	523	287	1743		1.5	2.8	16.6		1.5	4.3	20.9		KH
689880	792789	223	28	220	1327	350	1876		1.1	5.5	22.7		1.1	6.6	29.3		KH
689731	792789	215	29	211	458	1456			1.2	8.9			1.2	10.1			A
689712	792789	214	30	36	365	622	1478		0.8	6.5	11.2		0.8	7.3	18.5		AA
690455	794011	211	31	102	448	2322			0.9	10.4			0.8	11.2			A
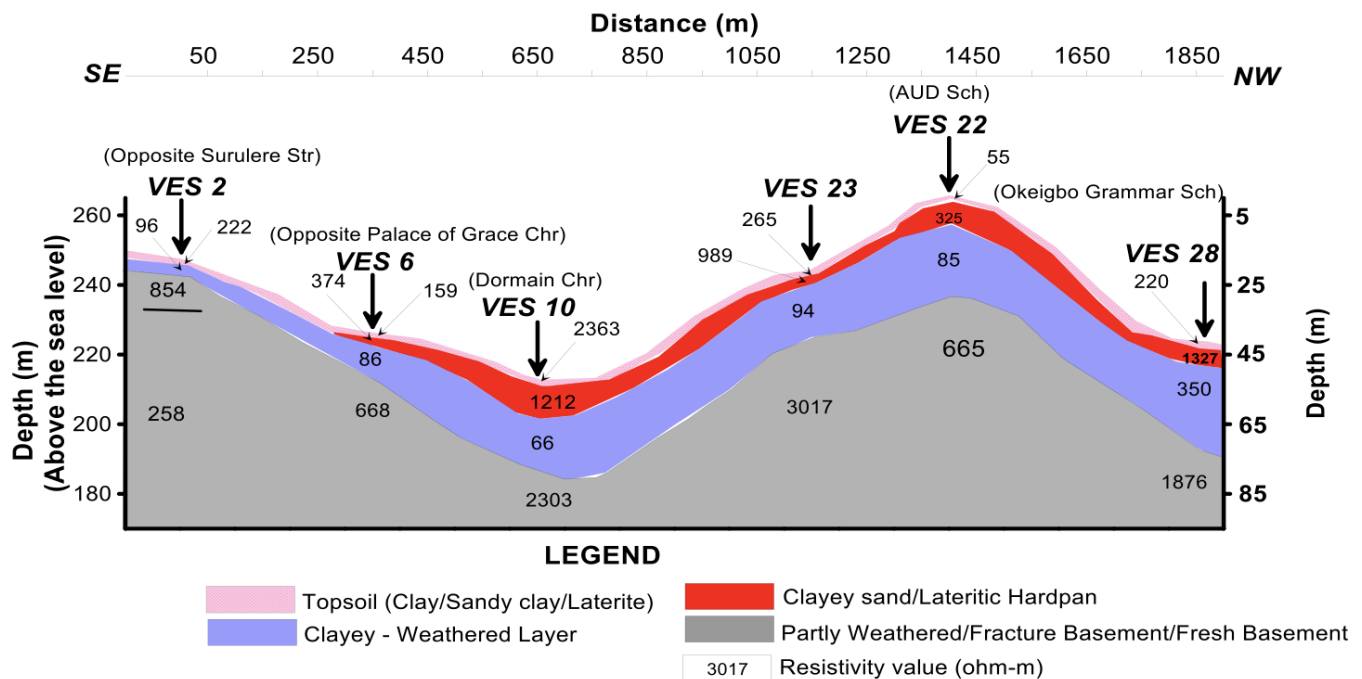
Figure 11. Geologic Section/Profile along the selected VES point established in the study area

The weathered layer has resistivity ranging between 38 ohm-m and 1202 ohm-m (avg. 240 ohm-m), indicating clayey weathered layer; the thickness ranged from 4.2 m and 25.5 m (avg. 14.1 m). The fractured basement was delineated under VES 4, and has resistivity of 226 ohm-m with thickness of 8.3 m. The depths to basement rock varied from 8.2 – 31.5 m (avg. 20.9 m), indicating moderate/thick weathering profile, and resistivity ranging from 258 – 4520 ohm-m (avg. 2035 ohm-m). Typical section shown in Figure 7 are characterized by topsoil (55 – 2363 ohm-m), subsoil (374 – 1327 ohm-m), weathered layer (66 – 350 ohm-m), fractured basement (258 – 854 ohm-m) and basement rock (1876– 2303 ohm-m). The relief of the basement is rugged which can aid groundwater accumulation. The spatial distribution map of weathered layer resistivity, thickness, overburden thickness, and traverse resistance are shown in Figure 10. The weathered layer resistivity in Figure 10a showed values generally less than 150 ohm-m especially (clay/sandy clay) in the central part, while values in the range of 150 – 250 ohm-m (sandy clay/clay sand) are common in the northern and southern areas; with highest thickness of 17.4 – 24.2 m found in the central part (Figure 10b). The overburden thickness of the area ranged from 4.2 – 31.5 m with regional average of 20.0 m, with quartzite, quartz schist, and metadiorite recorded averages of 18.3 m, 20.1 m, and 17.3 m respectively; hence the overburden thickness is higher in quartz schist and quartzite environment. The overburden thickness in the range of 22 – 31 m is the most dominant (Figure 9c). The spatial variation of the overburden thickness is shown in Figure 9c, showed dominant thickness ranging from 23 – 29 m. In the basement complex of southwestern Nigeria, overburden thickness above 15 m is usually considered thick and prolific for groundwater accumulation, hence are zones of high groundwater potential. Therefore priority most be given to those zones during groundwater development scheme. Although the nature of the overburden in terms of resistivity, transmissivity, hydraulic conductivity, sorption and hydraulic gradient are also important parameters in deciphering overall water yield of the weathered layer (Falowo, 2022). Consequently, the central part showed more potential in terms of aquifer thickness and transverse resistance than other part of the study area.

The summary of aquifer units' geology and its geoetectrical parameters, overburden thickness, hydraulics characteristics, and vulnerability are presented in Table 2. The traverse resistance ranged from 483.2 to 26337.3 Ωm^2 (avg. 4965.575 Ωm^2). The transverse resistance in the range of 5000 – 8500 ohm-m^2 and 8500 - 11500 ohm-m^2 (Figure 10d) characterized the southern and central zone respectively. The average values estimated for different geological units in the area: quartzite, quartz schist and metadiorite are 8578 Ωm^2, 8454 Ωm^2, and 9916 Ωm^2 respectively, with metadiorite having the highest value (Table 2). Lower TR values less than 5000 ohm-m^2 are areas with low yield/potential, values ranging from 5000 – 10000 ohm-m^2 are moderate groundwater potential area, while values above 10000 ohm-m^2 are high prospect zones (Falowo, 2022). Consequently, the study has moderate groundwater potential.
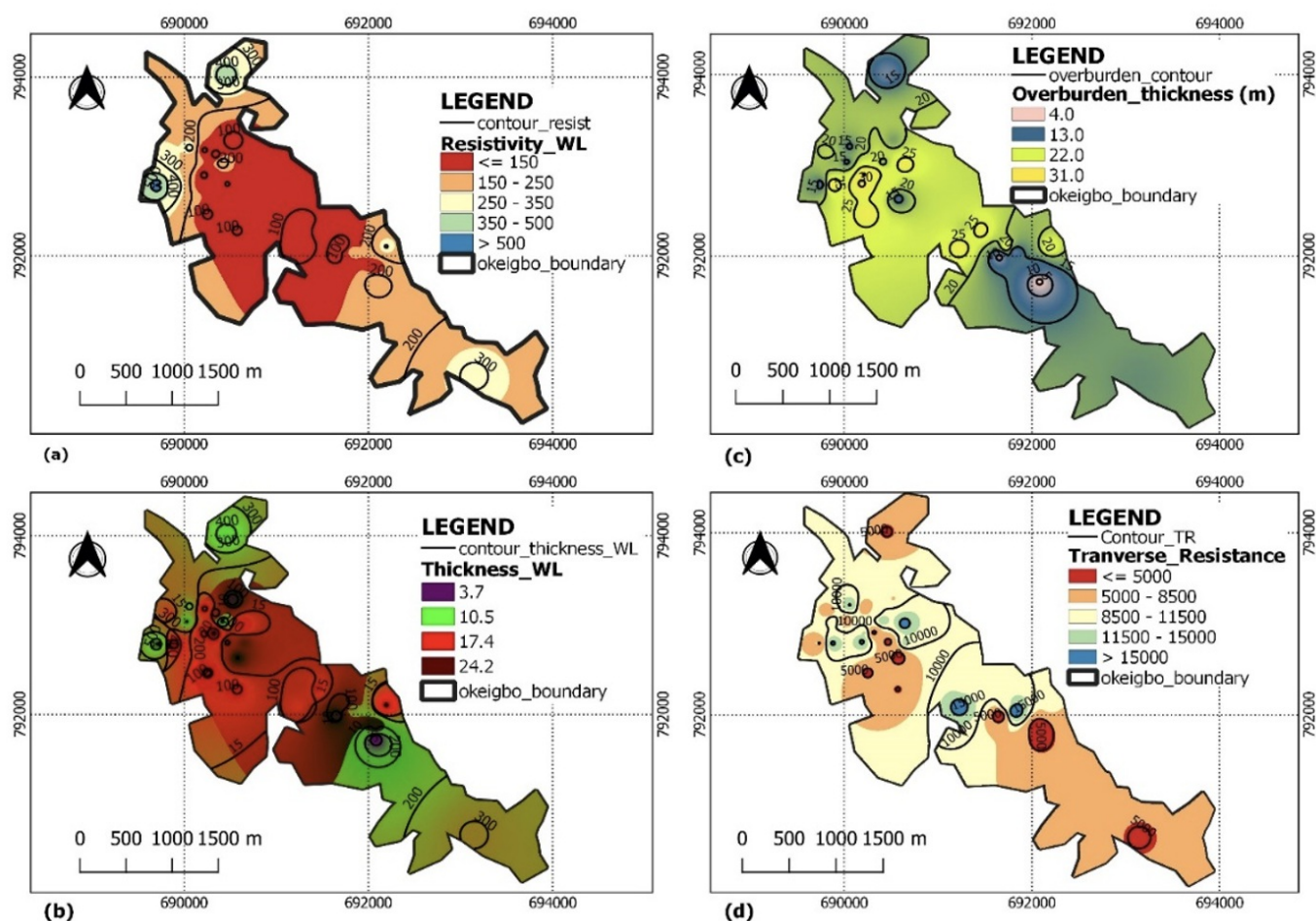
Figure 12. The spatial distribution of (a) weathered layer resistivity, (b) weathered layer thickness, (c) overburden thickness, and (d) transverse resistance

Table 2 showed the data calculated for aquifers' hydraulic characteristics, and longitudinal unit conductance values for the study area. The geology of the area where the VESs were conducted are quartzite (constitutes 29 % of the VES area), quartz schist (35.5 %), and metadiorite (35.5 %). The estimated hydraulic conductivity (HC) obtained ranged from 0.23 – 0.52 m/d (0.42 m/d) which suggests clay sand and corroborates the electrical resistivity result; while average of 0.23 m/d, 0.52 m/d, and 0.48 m/d were recorded for quartzite, quartz schist, and metadiorite respectively. The transmissivity of an

aquifer is explained as the rate at which water flows through the aquifer under a unit width and a unit hydraulic gradient. The hydraulic conductivity of an aquifer is described as the pace at which the water flows in the aquifer.

Table 2. Summary of aquifer units' geology, hydraulics characteristics, and vulnerability

VES No.	Aquifer Unit				Overburden Thickness (m)	S (Ω^{-1})	T (Ωm^2)	K (m/day)	T (m^2/day)	Fc	Rc	Fm	PT	PL	λ
	Resistivity (Ωm)	Thickness (m)	Geology	Type											
1	312	14.2	Quartzite	Weathered layer	16.1	0.0556	4788	0.23	3.34	4.27	0.62	3.79	297.37	289.47	1.01
2	258	3.2	Metadiorite	Weathered/fracture Basement	4.2	0.0419	4072	0.48	1.53	0.30	-0.54	3.57	496.54	195.91	1.59
3	102	10.2	Quartz schist	Weathered layer	13.5	0.1379	1574	0.52	5.34	20.70	0.91	5.93	116.62	97.90	1.09
4	185	13.9	Quartzite	Weathered/fracture Basement	12.3	1.6979	19625	0.23	3.27	9.15	0.87	3.79	749.06	309.15	1.56
5	302	19.7	Quartzite	Weathered layer	24.4	0.0754	9189	0.23	4.63	7.48	0.76	3.79	376.59	323.54	1.08
6	86	8.9	Metadiorite	Weathered layer/fracture Basement	8.9	0.1219	1965	0.48	4.26	7.77	0.77	3.57	148.87	108.33	1.17
7	55	12.3	Metadiorite	Weathered layer	24.2	0.2408	10964	0.48	5.89	20.24	0.91	3.57	453.05	100.48	2.12
8	112	17.8	Quartz schist	Weathered layer	27.3	0.1698	10881	0.52	9.31	22.60	0.92	5.93	398.56	160.75	1.57
9	47	15.3	Quartz schist	Weathered layer	20.7	0.3341	10908	0.52	8.00	26.30	0.93	5.93	526.96	61.95	2.92
10	66	16.3	Quartz schist	Weathered layer	27.5	0.2552	17528	0.52	8.53	34.89	0.94	5.93	637.37	107.76	2.43
11	126	12.2	Metadiorite	Weathered layer	20.7	0.1219	12719	0.48	5.85	26.21	0.93	3.57	614.42	169.82	1.90
12	144	19.9	Quartz schist	Weathered layer	28.6	0.1726	17118	0.52	10.41	23.35	0.92	5.93	598.52	165.71	1.90
13	38	8.2	Metadiorite	Weathered layer	17.3	0.2316	8432	0.48	3.93	96.11	0.98	3.57	487.42	74.70	2.55
14	265	9.7	Metadiorite	Weathered layer	19	0.0536	13882	0.48	4.65	7.94	0.78	3.57	730.63	354.46	1.44
15	69	14.1	Metadiorite	Weathered layer	21.9	0.2226	8742	0.48	6.76	52.86	0.96	3.57	399.19	98.40	2.01
16	88	19.3	Quartz schist	Weathered layer/fracture Basement	19.3	0.2307	6030	0.52	10.10	10.22	0.82	5.93	247.14	105.75	1.53
17	95	13.4	Quartz schist	Weathered layer	23.8	0.1887	3935	0.52	7.01	23.28	0.92	5.93	165.33	126.11	1.15
18	111	25.5	Quartzite	Weathered layer	27.9	0.2340	4357	0.23	5.99	19.79	0.90	3.79	156.15	119.25	1.14
19	78	19.8	Quartzite	Weathered layer	30.2	0.2813	12021	0.23	4.65	57.95	0.97	3.79	398.05	107.35	1.93
20	123	15.4	Metadiorite	Weathered layer	31.5	0.1446	15654	0.48	7.38	24.37	0.92	3.57	496.95	217.86	1.51
21	101	9.9	Quartzite	Weathered layer	13	0.1101	2628	0.23	2.33	12.10	0.85	3.79	202.12	118.05	1.31
22	85	20.5	Quartzite	Weathered layer/fracture Basement	28.7	0.2785	4192	0.23	4.82	7.82	0.77	3.79	146.05	103.06	1.19
23	94	18.4	Quartzite	Weathered layer	22.5	0.2032	4916	0.23	4.32	32.10	0.94	3.79	218.48	110.73	1.40
24	323	12.3	Metadiorite	Weathered layer/fracture Basement	14.2	0.0211	15117	0.48	5.89	0.27	-0.58	3.57	1064.58	673.30	1.26

25	258	9.9	Metadiorite	Weathered layer	14.2	0.0660	6096	0.48	4.74	8.30	0.78	3.57	429.32	215.18	1.41
26	285	14.8	Metadiorite	Weathered layer/fracture Basement	18.9	0.0628	11431	0.48	7.09	3.12	0.51	3.57	604.80	300.97	1.42
27	287	16.6	Quartz schist	Weathered layer	20.9	0.0699	6566	0.52	8.68	6.07	0.72	5.93	314.17	299.17	1.02
28	350	22.7	Quartzite	Weathered layer	29.3	0.0740	15486	0.23	5.33	5.36	0.69	3.79	528.52	395.94	1.16
29	458	8.9	Quartz schist	Weathered layer	10.1	0.0251	4329	0.52	4.66	3.18	0.52	5.93	428.65	402.08	1.03
30	622	11.2	Quartz schist	Weathered layer	18.5	0.0580	9368	0.52	5.86	2.38	0.41	5.93	506.36	318.76	1.26
31	448	10.4	Quartz schist	Weathered layer	11.2	0.0320	4751	0.52	5.44	5.18	0.68	5.93	420.44	352.71	1.09
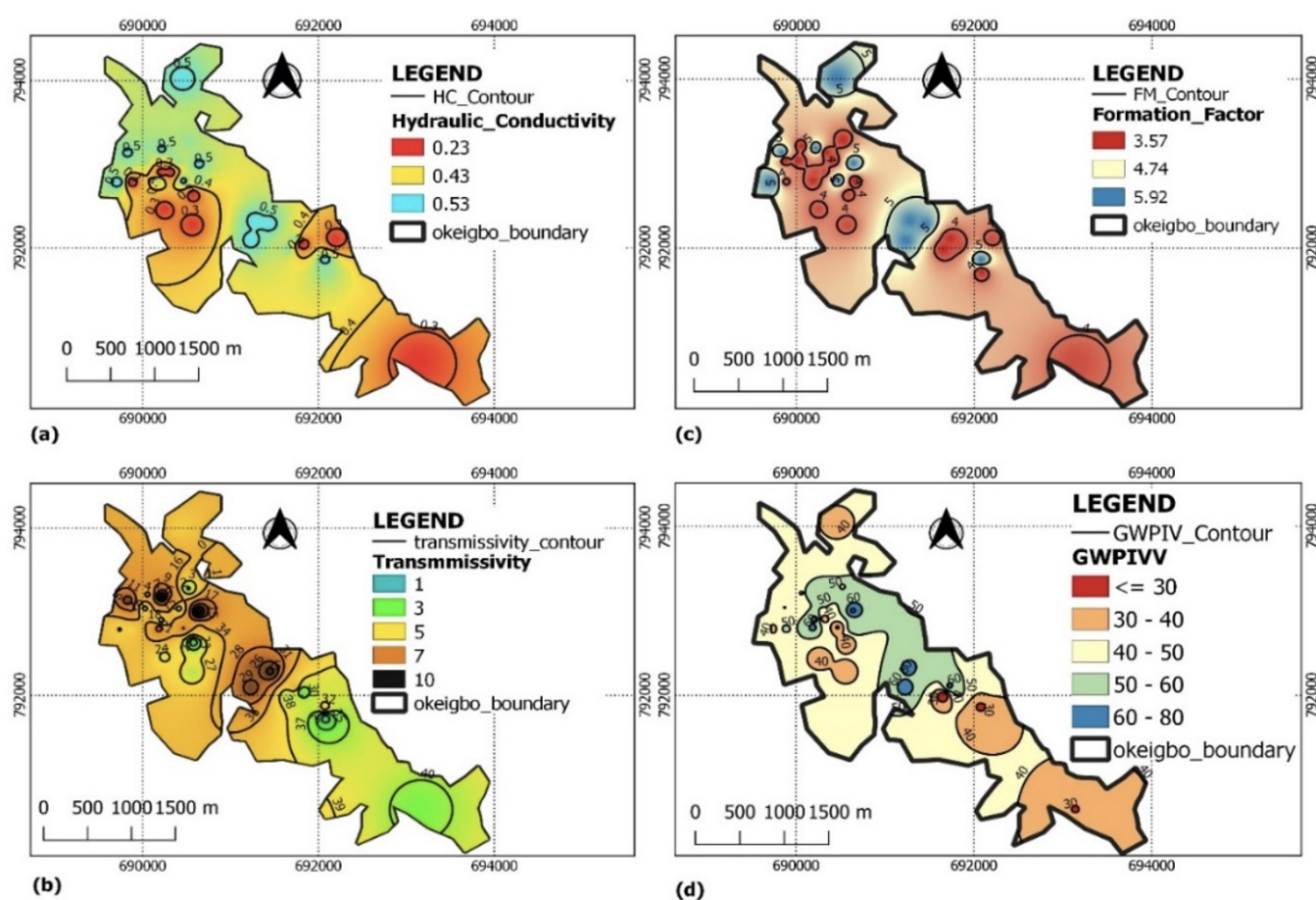
Figure 13. The spatial distribution of (a) hydraulic conductivity, (b) transmissivity, (c) formation factor, and (d) groundwater potential index values
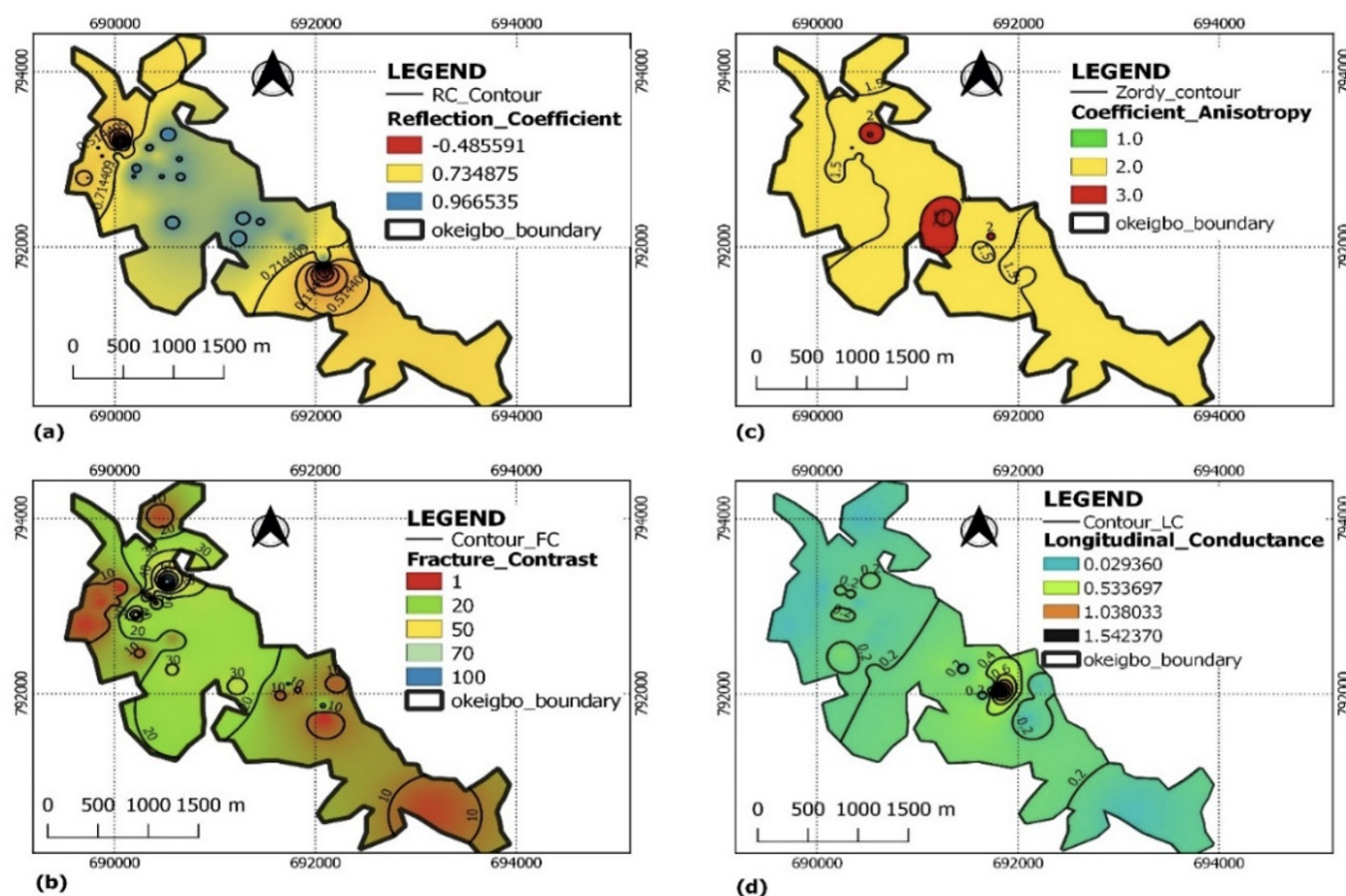
Figure 14. The spatial distribution of (a) reflection coefficient, (b) fracture contrast, (c) Zordy coefficient or electrical anisotropy, and (d) longitudinal conductance

The transmissivity (T) varied between 1.53 to 10.41 m^2/d (with regional average of 5.81 m^2/d), while the respective geologic units ranged from quartzite: 2.33 – 5.99 m2/d (4.30 m^2/d avg.), quartz schist: 4.66 – 10.41 m^2/d (7.58 m^2/d avg.), metadiorite: 1.53 – 7.38 m2/d (5.27 m^2/d avg.), with quartz schist showing better potential on the basis of HC and T. The spatial distribution of HC and T in Figure 11a & b showed northern and mid-central parts with better hydraulic properties, with HC and T ranging from 0.43 – 0.53 m/d, and 5 – 10.0 m/d respectively. However using the criteria in Table 7 the T values fall within low zone since the values are less than 10 m2/d. The fracture contrast and reflection coefficient is between 0.27 – 96.11 (18.76 avg.) and -0.58 to 0.98 (0.73 avg.). The average FC and RC values obtained for quartzite are 17.34 and 0.82; 16.20 and 0.79 (quartz schist), and 22.5 and 0.58 (metadiorite). The Fracture contrast and reflection coefficient have strong relationship with groundwater yield, as high FC implies high groundwater potential; and low RC indicates high groundwater yield.

The spatial distribution map of RC and FC is shown in Figure 12, the mid central and the north central are characterized with relatively high RC of 0.73 – 0.97, the extreme northern part and southern area have low RC values (less than 0.73); while the FC is generally less than 50. These range of values imply high groundwater yield or propensity zones characterized with weathered or partly weathered/fracture basement saturated aquifer especially in the mid central and north central parts. The formation factor (F_M) ranged from 3.57 (metadiorite) – 3.79 (quartzite) and 5.93 (quartz schist) and

average value of 4.47. Formation factor has good positive correlation with groundwater yield, therefore quartz schist and quartzite showed better tendency, although the recorded range of values is low for high prolific aquifer that is capable of providing all year needs of water supply. Hence using Table 7, the area is of moderate groundwater yield. The transverse (P_T) and longitudinal (P_L) resistivity ranged from 116.62 – 1065 (430 avg.) and 61.95 – 673 (212 avg.) respectively, while the geologic units recorded average values of 341 and 209 (quartzite); 539 and 228 (metadiorite); and 396 and 200 (quartz schist). The Zordy coefficient of anisotropy or electrical anisotropy (λ) ranged between 1.01 and 2.92 (avg. 1.52); while averages of 1.31, 1.55, and 1.67 were recorded for quartzite, quartz schist, and metadiorite. Using Table 7, based on the overall average value of 1.52, the area has high prospect; while quartz schist, quartz schist, and metadiorite showed lesser prolificacy in that order. Figure 12d showed the spatial variation of λ, with values generally less than 3.0, although two spots of high λ are observed in the northeastern and mid-central parts. The λ determines the degree of fracturing or inhomogeneity of subsurface geology in relation to groundwater accumulation or yield potential, as the higher the λ, the higher the groundwater yield.

Open well/Borehole Aquifer Hydraulic Characterization

The hydrogeologic measurements helps in groundwater prediction and availability by determination of water column, static water level, and hydraulic head. This information can be used to assess location and thickness of water zone, their confinement, and hydrogeological margins; the levels of water and their variations with seasons (time); their storage potential and transmissivity (Subbao Rao, 2017). Hydraulic information was taken from six boreholes and eleven open wells, and some of the wells coincided with the location of the VES's stations, as presented in Tables 3 and 4. The information from the boreholes presented total depth ranging from 25 – 35 m (30 m avg.) and SWL ranging from 10 – 18 m (avg. 13.8 m) signifying moderately deep aquifer. The geologic section observed from four borehole cuttings is shown in Figure 13, the cuttings were visually inspected in their natural state or condition. The geologic layers observed from the sites investigated and their depths range are clay/lateritic clay (2.5 – 7.5 m), sandy clay (2.5 – 15.5 m), clayey sand (3.0 – 27.5 m), clay-sand mixture (18.0 – 28.5 m) and basement rock 24.5 (quartz schist) – 33.5 m (quartzite). The static water level ranged between 10.5 (BH 04; quartz schist) – 18.5 m (BH 01; quartzite). Consequently the SWL is moderately deep in the study area, with clay-sand mixture being the major aquifer (weathered zone).

The data acquired from eleven (11) one across three different rocks is presented in Table 4. The total depth the wells ranged from 5.2 – 10.1 (7.5 avg.) in quartzite, SWL ranged from 2.2 (metadiorite) – 6.5 m (quartzite) with average of 4.1 m, while the water column is between 1.3 (quartzite) – 4.8 m (metadiorite) with average of 3.4 m, the hydraulic head varied between 215.1 to 244.9 m (233.2 m avg.). The thickness of the vadose zone which corresponds to the static water level (SWL) is generally low i.e. less 5 m, which may not be capable of providing sufficient protection for the aquifer. The hydraulic conductivity, transmissivity, and storativity was obtained from the pumping test, with typical pumping test data and their corresponding curves are shown in Table 5 and Figure 14. The HC ranged from 0.23 (quartzite) to 0.52 m/d (metadiorite) (0.43 m/d avg.); transmissivity varied from 1.22 m^2/d (quartzite) – 5.13 m^2/d (quartz schist) with average value of 3.17 m^2/d. The pore water resistivity (PWR) varied from 33.9 (quartzite) – 39.68 ohm-m (quartz schist) and average of 36.65 ohm-m, the formation factor ranged from 2.55 (quartzite) to 6.55 (quartz schist) (4.49 avg.), the storativity (Sr) varied from 0.13402 (quartzite) to 5.22388 (quartz schist). The regression model (equation 12) was used to predict the storativity

especially in locations where pumping test was not carried. The empirical relationship between transmissivity and storativity, gives high positive linear correlation of 0.999. Typical field curves of some the wells is shown in Figure 14. Storativity is the product of the specific storage and the aquifer thickness. Consequently, the average storativity (Sr) or coefficient of storativity is greater than 0.005 which suggests an unconfined aquifer. The results of the well hydraulics correlate well with those estimated for the VES locations.

$$\text{Storativity} = 1.046(x) - 0.1421 \qquad (12)$$

Where x is transmissivity

Table 3. Summary of Well Information and Sample Locations

East	North	Borehole No.	Elevation (m)	Total Depth	SWL	Geology	Present State
691102	792500	BH-1	216	35	18	Quartzite	Functioning
692371	791573	BH-2	249	28	12	Quartz schist	Functioning
692183	791442	BH-3	245	32	15	Quartz metadiorite	Functioning
692602	791175	BH-4	245	25	10	Quartz schist	Functioning
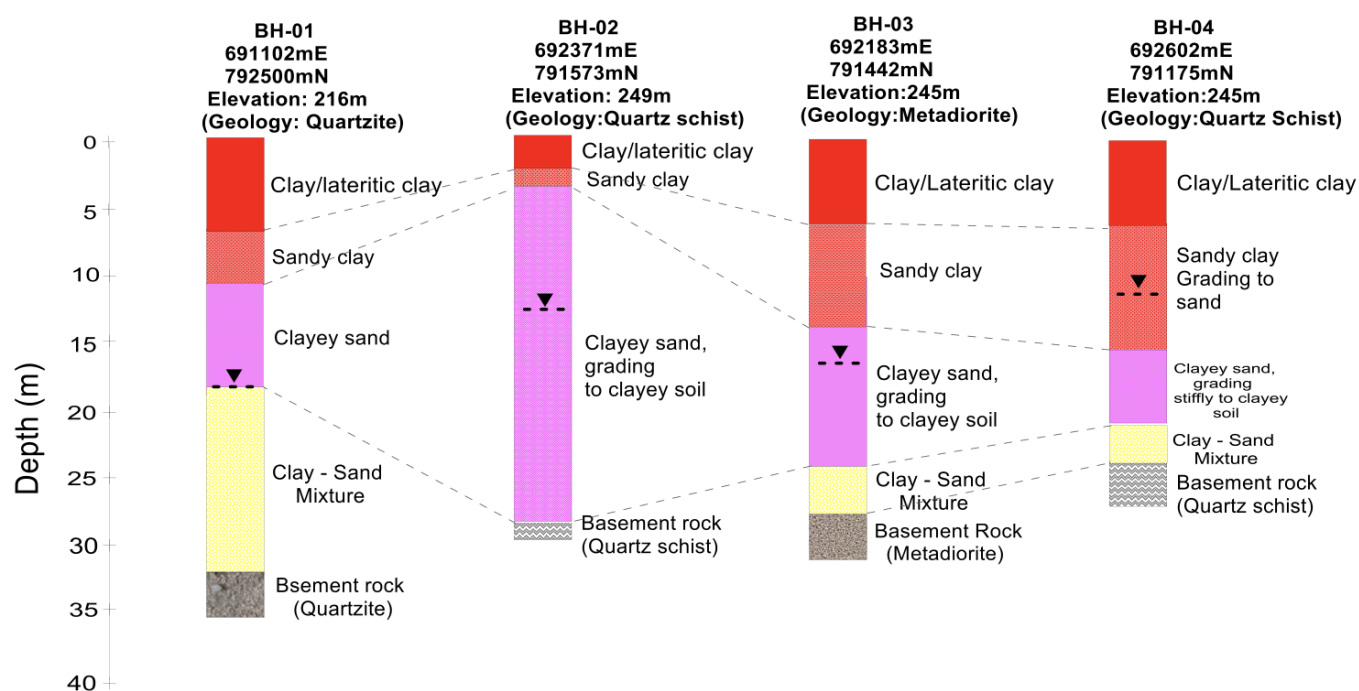
Figure 15. Borehole sections showing the various geologic units observed from borehole cuttings

Table 4. Summary of Well Information from three geological units

East	North	WLN	Elev (m)	TD (m)	SWL (m)	WC (m)	HH (m)	K (m/d)	T (m²/d)	Geology	PWR (ohm-m)	Sr	F$_M$
690939	792858	WL-1	219	5.2	3.9	1.3	215.1	0.23	1.22	Quartzite	33.90	1.13402	6.08
690972	792637	WL-2	222	5.5	2.8	2.7	219.2	0.52	2.88	Quartz schist	34.84	2.87038	5.80
691890	792066	WL-3	233	7.8	4.1	3.7	228.9	0.48	3.74	Metadiorite	37.74	3.76994	2.68
691777	792231	WL-4	227	9.3	4.5	4.8	222.5	0.48	4.46	Metadiorite	36.90	4.52306	2.71
692313	791690	WL-5	250	8.2	5.1	3.1	244.9	0.23	1.93	Quartzite	36.10	1.87668	2.71
692110	791582	WL-6	246	5.9	2.2	3.7	243.8	0.48	2.83	Metadiorite	35.34	2.81808	3.23
692196	791410	WL-7	245	8.5	3.9	4.6	241.1	0.48	4.07	Metadiorite	37.88	4.11512	5.68
692505	791188	WL-8	246	10.1	6.5	3.6	239.5	0.23	2.37	Quartzite	37.31	2.33692	2.55
692795	791430	WL-9	247	9.8	5.4	4.4	241.6	0.52	5.13	Quartz schist	34.36	5.22388	6.55
692094	790911	WL-10	234	5.8	3.0	2.8	231	0.52	3.03	Quartz schist	39.68	3.02728	5.54
692179	791221	WL-11	241	6.2	3.3	2.9	237.7	0.52	3.24	Quartz schist	39.06	3.24694	5.89

WLN - Well No., Elev- Elevation, TD- Total depth, SWL – Static water level, WC – Water column, HH – Hydraulic head, K – Hydraulic conductivity, T – Transmissivity, PWR – Pore water pressure, Sr – Storativity, FM – Formation factor
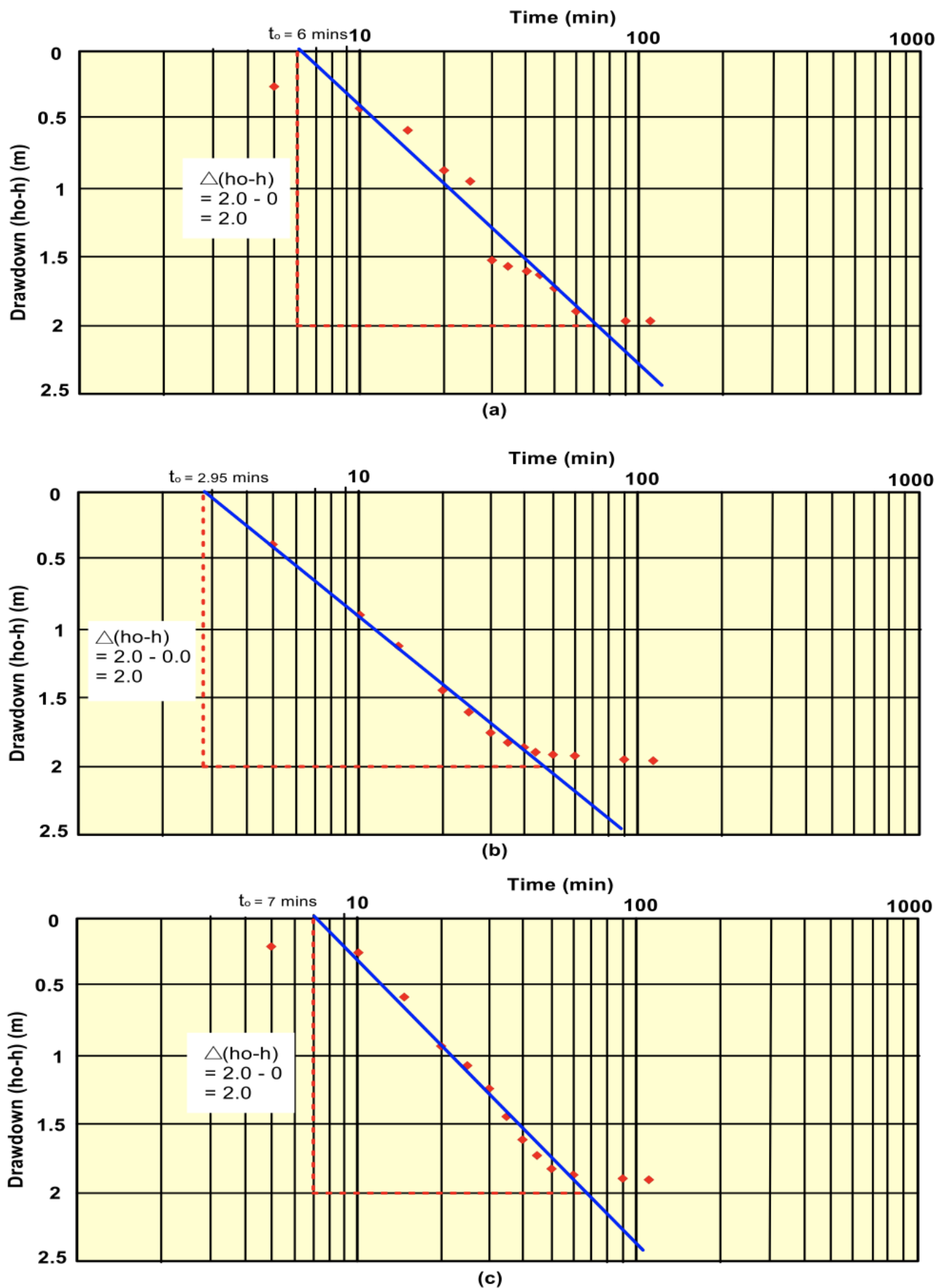
Figure 15. Typical pumping test curves for wells across the three geological units (a) W-1 -quartzite (b) W-2 – quartz schist (c) W-7- metadiorite.

Hydrogeological Parameters Modeling and Groundwater Potential Mapping

Empirical model was developed for the three geological units (quartzite, quartz schist, metadiorite), by plotting formation factor on x-axis and hydraulic conductivity on y-axis. All the rock units showed positive correlations however quartz schist is much stronger (0.7076) than quartzite (0.2957) and metadiorite (0.3517) as shown in Table 5. The modeling of aquifers' potentiality zones was done using groundwater potential index values (GWPIV) to produce groundwater potential map (Falowo, 2022; Bawallah et al., 2019) in Figure 10d and the obtained values for all rated parameters are shown in Table 7. The GWPIV has proved been identified as one of the veritable tools in groundwater assessment and management. Therefore, in this study, multi-criteria decision analysis (MCDA) was done using analytical hierarchy process (AHP) (Saaty, 1980, 1990). The AHP is a theory of measurement for dealing with quantification and/or intangible criteria that has found rich applications in decision theory, conflict resolution and in models of the brain (Vargas, 1990). The decision applications of the AHP are carried out in two phases: hierarchic design and evaluation using paired comparisons. The normal procedure for AHP was involved in this study by prioritizing the hydrogeologic parameters according to their importance in groundwater accumulation; then the parameters are pair-wise in a matrix form using Saaty (1980) scale of importance, where 1, 3, 5, 7, and 9 are equal, moderate, strong, very strong, and extreme importance respectively; while 2, 4, 6, and 8 are intermediate values; and 1/3, 1/5, 1/7, and 1/9 are values for inverse comparison.

The average values of the relative values in every row are determined, and this gives the criteria weights; consequently the consistency ratio was determined by multiplying the pair-wise comparison matrix with criteria weights calculated for each row, and the average value determined to obtain the weighted sum value. Thereafter, the weighted sum value is divided by criteria weights to obtain consistency ratio for each of the rows. Hence, the average consistency ratio is obtained as Lambda (λ_{max}). The next is the determination of consistency index (CI) using equation 13. It is the consistency index of a pairwise comparison matrix which is generated randomly, random index depends on the number of elements which are compared as shown in Table 6.

$$CI = \frac{\gamma_{max} - n}{n - 1} \qquad (13)$$

Where n is the number of parameters compared.

The criteria weight was tested to know its accuracy, reliability, credibility, and consistency in predicting groundwater yield in the study area by dividing the CI with random consistency index value obtained in Table 6 and the resulted value must be less than 0.10, which is the rule of the process. The obtained weights (w) were used to rate the parameters accordingly (Table 7) as AQT - aquifer layer thickness (0.07), AQR - aquifer layer resistivity (0.16), OVT - overburden thickness (0.10), TR - transverse resistance (0.20), TMY - transmissivity (0.26), CoA - coefficient of anisotropy (0.22). In generating groundwater potential index values (GWPIV), the rating (r) obtained from AHP was multiplied with the weights (which varied from 1 to 5) based on their degree of relevance in groundwater storage and utilization (Table 7), and were summed up (equations 14-15).

$$GW = f(AQT,\ AQR,\ OVT,\ TR,\ TMY,\ COA) \qquad (14)$$

Therefore the GWPIV was determined using the expression below:

$$GWPIV = AQT_w AQT_r + AQR_w AQR_r + OVT_w OVT_r + TR_w TR_r + TMY_w TMY_r + COA_w COA_r \qquad (15)$$

Thematic layers of the parameters were generated using QGIS software; and the same software was used to do the classification, and produced the GWPIV and subsequent groundwater potential map. The GWPIV was ranked as very low: 0.0 – 1.0; low: 1.0 – 2.0; moderate: 2.0 – 3.0, high: 3.0 – 4.0, and very high greater than 4. Thus the GWPIV ranged from metadiorite 1.08 (VES 06; weathered/fracture aquifer) – quartz schist 3.55 (VES 12; weathered aquifer) with an average of 2.35 indicating moderate groundwater potential. The developed groundwater potential map (Figure 11d) distinguished the area into three major potential zones, with prominent moderate zone (i.e. GWPIV: 40 – 50 %) constituting 55 % of the study area.

Table 5. Empirical Relationship between hydraulic conductivity and formation factor for different water bearing formations derived geological units

S/Nos.	Geological units	Exponential Equation	Correlation coefficient
1	Quartz schist	$y = 0.1029e^{0.2741x}$	0.7076
2	Quartzite	$y = 0.4543e^{-0.174x}$	0.2957
3	Metadiorite	$y = 0.3482e^{0.0894x}$	0.3517

Table 6. Random Consistency Index Table for number of parameter (N) and corresponding random value (Saaty, 2006)

N	1	2	3	4	5	6	7	8	9	10
RV	0	0	0.52	0.89	1.11	1.25	1.35	1.40	1.45	1.49

Table 7. Probability rating, normalized weight for different classes of parameters used in deriving the GWPIV

	Parameter	Range	Weight	Remark	Rating
1	Aquifer Layer Thickness (m)	0 – 5	1	Very Low	0.05
		6 – 10	2	Low	
		11 – 15	3	Moderate	
		16 - 20	4	High	
		>20	5	Very High	
2	Aquifer Layer Resistivity (ohm-m)	1 – 100 (Clay)	1	Very Low	0.04
		101 – 250 (Sandy clay)	2	Low	
		251 – 350 (Clayey sand)	3	Moderate	
		351 – 750 (Sand/Fractured aquifer)	5	Very High	
3	Overburden Thickness (m)	1 – 10	1	Low	0.12
		11 – 20	2	Medium	
		21 – 30	3	High	
		>30	5	Very High	
4	Transverse Resistance (ohm-m^2)	1 – 5000	1	Low	0.18
		5001 – 10000	3	Fair	
		>10000	5	High	
5	Transmissivity (m^2/d)	1 – 10	1	Low	0.32
		11 – 20	3	Moderate	
		>20	5	High	
6	Coefficient of Anisotropy	1.1 – 1.15	1	Very Low	0.25
		1.15 – 1.19	2	Low	
		1.19 – 1.25	3	Moderate	
		1.25 – 1.30	4	High	
		1.30 – 2.0	5	VeryHigh	

Table 8. Summary of the obtained values for the seven parameters pair-wise and resulted GWPIV

East	North	VES No.	AQR	AQT	OVT	TR	T	COA	GWPIV	GWPIV (%)
693140	790657	1	0.3	0.21	0.32	0.2	0.26	0.22	1.51	29.9
692082	791725	2	0.3	0.07	0.16	0.2	0.26	0.66	1.65	32.7
692076	791863	3	0.2	0.21	0.32	0.2	0.26	0.22	1.41	27.9
691822	792048	4	0.2	0.21	0.32	1	0.26	0.66	2.65	52.5
692193	792104	5	0.3	0.28	0.48	0.6	0.26	0.22	2.14	42.4
691655	791991	6	0.1	0.14	0.16	0.2	0.26	0.22	1.08	21.4
691729	792114	7	0.1	0.21	0.48	1	0.26	1.1	3.15	62.4
691451	792288	8	0.2	0.28	0.48	1	0.26	0.66	2.88	57.0
691278	792329	9	0.1	0.28	0.48	1	0.26	1.1	3.22	63.8
691234	792094	10	0.1	0.28	0.48	1	0.26	1.1	3.22	63.8
690653	792799	11	0.2	0.21	0.48	1	0.26	0.88	3.03	60.0
690641	793004	12	0.2	0.28	0.48	1	0.78	0.88	3.62	71.7
690523	793280	13	0.1	0.14	0.32	0.6	0.26	1.1	2.52	49.9
690412	793040	14	0.3	0.14	0.32	1	0.26	0.44	2.46	48.7
690344	793132	15	0.1	0.21	0.48	0.6	0.26	1.1	2.75	54.5
690220	793183	16	0.1	0.28	0.32	0.6	0.78	0.66	2.74	54.3
690467	792804	17	0.1	0.21	0.48	0.2	0.26	0.22	1.47	29.1
690319	792907	18	0.2	0.35	0.48	0.2	0.26	0.22	1.71	33.9
690214	792902	19	0.1	0.21	0.8	1	0.26	0.88	3.25	64.4
690189	792804	20	0.2	0.28	0.8	1	0.26	0.66	3.2	63.4
690579	792636	21	0.2	0.14	0.32	0.2	0.26	0.44	1.56	30.9
690251	792467	22	0.1	0.35	0.48	0.2	0.26	0.22	1.61	31.9
690572	792283	23	0.1	0.28	0.48	0.2	0.26	0.44	1.76	34.9
690059	793208	24	0.3	0.21	0.32	1	0.26	0.44	2.53	50.1
690028	793040	25	0.3	0.14	0.32	0.6	0.26	0.44	2.06	40.8
689873	793040	26	0.3	0.21	0.32	1	0.26	0.44	2.53	50.1
689836	793132	27	0.3	0.28	0.48	0.6	0.26	0.22	2.14	42.4
689880	792789	28	0.3	0.35	0.48	1	0.26	0.22	2.61	51.7
689731	792789	29	0.5	0.14	0.32	0.2	0.26	0.22	1.64	32.5
689712	792789	30	0.5	0.21	0.32	0.6	0.26	0.44	2.33	46.1
690455	794011	31	0.5	0.21	0.32	0.2	0.26	0.22	1.71	33.9

The low potential zone (i.e. GWPIV: 30 – 40 %) are conspicuous in the southern part and constitute 25 % of the study area; while the high potential zone (20 % of the study area) are common in the mid-central and north central parts. Therefore the synthesis of all the parameters culminating in GWPIV, proved and corroborated the earlier results, which showed high or better groundwater potential in quartz schist and quartzite areas than metadioritic environment. However, the longitudinal unit conductance (LUC) recorded values ranging from 0.0211 – 1.6979 mhos (with regional average of 0.19396 mhos); while quartzite recorded 0.0556 – 1.6979 mhos (0.33444 mhos avg.); quartz schist (0.0251 – 0.3341 mhos; 0.15218 mhos

avg.); and metadiorite recorded 0.0211 – 0.2408 mhos (0.1208 mhos avg.). Using Table 9, the groundwater system in the study area is weak, although the central appears less weak, as shown in spatial distribution map of LUC in Figure 12d.

Table 9. Longitudinal unit conductance and corresponding protective rating (Falowo, 2022)

Total Longitudinal unit Conductance (mhos)	Rating of overburden's aquifer protective capacity
<0.10	Poor
0.1 – 0.49	Weak
0.5 – 0.99	Moderate
1.0 - 4.99	Good
5.0 – 10.0	Very good
>10.0	Excellent

Conclusions

Multi-criteria decision analysis (MCDA) using Geographic Information System supported Analytical Hierarchy Process (AHP) has been undertaken in Okeigbo, Southwestern Nigeria. Six parameters of higher hydrogeologic importance were pairwise and weighted respectively: AQT - aquifer layer thickness (0.07), AQR - aquifer layer resistivity (0.16), OVT - overburden thickness (0.10), TR - transverse resistance (0.20), TMY - transmissivity (0.26), CoA - coefficient of anisotropy (0.22). Subsequently, the GWPIV ranged from metadiorite 1.08 (weathered/fracture aquifer) – quartz schist 3.55 (weathered aquifer) with an average of 2.35 indicating moderate groundwater potential; with the moderate zone (GWPIV: 40 – 50 %), low (GWPIV: 30 – 40 %), and high (i.e. GWPIV: above 50 %) constituted 55 %, 25 %, and 20 % of the study area. The high potential zone are common in the mid-central and north central parts. Conclusively, the quartz schist and quartzite areas showed better prolificacy than metadioritic environment. But in terms of protective capacity of the aquifers, the longitudinal unit conductance (LUC) regional average of 0.19396 mhos) showed weak protection of the aquifer as a result vertical infiltration and percolation of contaminants; while quartzite recorded 0.33444 mhos; quartz schist 0.15218 mhos; and metadiorite recorded 0.1208 mhos, hence quartzite is weak, quartz schist is weaker, and metadiorite being the weakest environment.

Nonetheless, the water table aquifer and the fracture basement are the major water bearing units in the area, and in some cases they occurred as combination. The drainage basin falls within the low – moderate regional drainage basins, with moderate to high flow connectivity and low – moderate flow direction. The area is well drained with major stream/river. The higher elevations are generally remarkable in the northern area (above 243 m), while the lower elevations characterized the southern area. This implies that there possibility of movement of water towards the northern part with the southern forming the watershed. Although spots of relatively high elevations are also observed in southern region. In addition, the hill shade showed varying forms of altitude with the range of 1 – 91 % most dominant; which infers that the altitude of the rock units or landforms varies from low – moderate and sloppy. The aspect which is the direction of the slope and range from 0 to 134.9

degrees. The result of GWPIV corroborated the terrain elevation drainage maps which showed the possibility of movement of water towards the northern part (discharged zone) with the southern forming the watershed. The drainage basin of the study area, and falls within the moderately low regional drainage basins with low –moderate flow connectivity. The drainage network and catchment area the maps revealed that all the channels serve as contributors to all the zones in the area, as all the major streams are generally interconnected, hence the catchment area for the area is large. The flow direction of the streams/rivers are generally lower in the northern area and higher in southern parts.

Acknowledgment

References

- Abdullahi, M.G., Toriman, M.E., Gasim, M.B., 2015, The Application of Vertical Electrical Sounding (VES) for Groundwater Exploration in Tudun Wada Kano State. Nigeria. Journal of Geology and Geosciences, 4(1), pp. 1–3.
- Adagunodo, M.K., Sunmonu, L.A., Aizebeokhai, A.P., Oyeyemi, K.D., Abodunrin, F.O., 2018, Groundwater Exploration in Aaba Residential Area of Akure, Nigeria. Front. Earth Science, 66(6), pp. 1–12, DOI:10.3389/feart.2018.00066.
- Aina, J.O., Adeleke O.O., Makinde V., Egunjobi, H.A., Biere, P.E., 2019, Assessment of Hydrogeological Potential and Aquifer Protective Capacity of Odeda, Southwestern Nigeria. RMZ – M&G, Vol. 66, pp. 199–210
- Akanbi, O.A., 2017, Hydrogeological Characterisation of Crystalline Basement Aquifers of part of Ibarapa Area, Southwestern Nigeria. Ph. D. Thesis. Ibadan-Nigeria: University of Ibadan 2017; 312 p.
- Akanji, A.A., Oni, A.G., Olorunfemi, M.O., 2021, Groundwater Prospectivity Assessment of a Field of Hand-Dug Wells in the Area Around the Murtala Muhammed Postgraduate Hall OAU, Ile-Ife, Using Geoelectric Parametric Soundings. The Pacific Journal of Science and Technology, Volume 22. Number 1. May 2021 (Spring)
- Alley, W.M., Leake, S.A. (2004). The journey from safe yield to sustainability. Groundwater, 42(1): 12-16. https://doi.org/10.1111/j.1745-6584.2004.tb02446.x
- Amadi, S.C., Onwuemesi, A.G., Anakwuba, E K., Chinwuko, A.I., Okeke, H.C., 2017, Estimation of Aquifer Hydraulic Characteristics from Surface Geo-Electrical Sounding of Affa and Environs Southeastern, Nigeria. IOSR Journal of Applied Geology and Geophysics (IOSR-JAGG), Volume 5, Issue 4 Ver. III (Jul. – Aug. 2017), pp. 21-32. DOI: 10.9790/0837-0504032132
- Anomohanran, O., 2013, Geophysical investigation of groundwater potential in Ukelegbe, Nigeria. J. Applied Sci., 13: 119-125. DOI: 10.3923/jas.2013
- ASCE Manual, 1987, Groundwater Management, American Society of Civil Engineers, New York.
- Bawallah, M.A., Aina, A.O., Ozegin, K.O., Akeredolu, B.E., Bamigboye, O.S., Olasunkanmi, N.K., Oyedele, A.A., 2019, Integrated Geophysical Investigation of Aquifer and Its Groundwater Potential in Camic Garden Estate, Ilorin Metropolis

North-Central Basement Complex of Nigeria. JAGG, 7(2), 01-08.

- Bayewu, O.O., Oloruntola, M.O., Mosuroa, G.O., Laniyana, T.A., Ariyo, S.O., Fatoba, J.O., 2018, Assessment of groundwater prospect and aquifer protective capacity using resistivity method in Olabisi Onabanjo University campus, Ago-Iwoye, Southwestern Nigeria. NRIAG Journal of Astronomy and Geophysics, 7, pp. 347–360.

- Bear, J., 1979, Hydraulics of Groundwater. McGraw-Hill Inc., New York

- Bisson, R.A., Lehr, J.H., 2004, Modern Groundwater Exploration. Wiley, New York.

- Brassington, R., 1988, Field Hydrogeology. Wiley, Chichester, 926pp.

- Chaanda, M.S., Alaminiokuma, G.I., 2020, Hydrogeophysical Investigation for Groundwater Resource Potential in Masagamu, Magama Area, Fractured Basement Complex, North-Central Nigeria. Malaysian Journal of Geosciences, 4(2): 43-47. DOI: http://doi.org/10.26480/mjg.02.2020.43.47

- Cosgrove, W.J., Loucks, D.P., 2015, Water Management: Current and Future Challenges and Research Directions. Water Resources Research, 51(6), pp. 4823–4839.

- Delleur, J., 1999, The Handbook of Groundwater Engineering. CRC Press LLC, USA.

- Driscoll, F.G., 1986, Groundwater and Wells. 2nd Ed. Johnson Division, St. Paul, 1089 p.

- Falowo, O.O., 2022, Modeling of hydrogeological parameters and aquifer vulnerability assessment for groundwater resource potentiality prediction at Ita Ogbolu, Southwestern Nigeria. Modeling Earth Systems and Environment, 21 pp. https://doi.org/10.1007/s40808-022-01490-8

- Falowo, O.O., Akindureni, Y., Ojo, O., 2017, Groundwater Assessment and Its Intrinsic Vulnerability Studies using Aquifer Vulnerability Index and GOD Methods. International Journal of Energy and Environmental Science, Vol. 2, No. 5, 2017, pp. 103-116. doi: 10.11648/j.ijees.20170205.13

- Falowo, O.O., Daramola, A.S., 2023, Geo-Appraisal of groundwater resource for sustainable exploitation and management in Ibulesoro, Southwestern Nigeria. Turkish Journal of Engineering 2023, 7(3), 236-258, DOI: 10.31127/tuje.1107329

- Falowo, O.O., Ojo, O.O., Daramola, A.S., 2020, Groundwater Resource Assessment by Hydraulic Properties Determination for Sustainable Planning and Development in Central Part of Ondo State, Nigeria. Environmental and Earth Sciences Research Journal Vol. 7, No. 1, March, 2020, pp. 1-8 https://doi.org/10.18280/eesrj.070101

- FAO/DSMW 2020. Digital Soil Map of the World at 1,500,000 Scale (Geonetwork). Food and Agricultural Organization https://www.fao.org/soils-portal/data-hub/soil-maps-and-databases/faounesco-soil-map-of-the-world/en/ Accessed 19th January, 2023

- Fetter, C.W., 2007, Applied hydrogeology. 2nd edition. USA: Merrill Publishing Company.

- Gao, Q., Shang, Y., Hassan, M., Jin, W., Yang, P., 2018, "Evaluation of a Weathered Rock Aquifer Using ERT Method in South Guangdong, China". Water. 10:1-22. https://doi.org/10.3390/w10030293

- Gogoi, U., 2013, Determination of aquifer parameters of the shallow aquifers of Barak valley, Assam, India. Int. Bulletin Water Resources Dev., 1: 1-13.

- Graham, M.T., Ball, D.F., Ó Dochartaigh, B.E., Irving, K., Simpson, E., 2006, Scottish Aquifer Properties, 2006 Interim Report, British Geological Survey Report Cr/06/073n.

- Hiscock, K.M., 2005, Hydrogeology: Principles and Practice. Blackwell Publishing, p.389

- Halford, K.J., Wright, W.D., Schreiber, R.P., 2006, Interpretation of Transmissivity estimates from singlewell pumping

aquifer tests. Ground Water, 44: 467- 471. DOI: 10.1111/j.1745-6584.2005.00151.x

- Harvill, Bell, F.G., 1986, Groundwater Resource Development, Butterworks, London.

- Iloeje, N.P., 1981, A New Geography of Nigeria. Longman Publisher Nigeria, pp. 201.

- Johnson, T., 2005, A measure of well performance, well problems and aquifer Transmissivity. WRD Technical Bulletin, 2: 1-2.

- Kruseman, G.P., de Ridder, N.A., 1991, Analysis and Evaluation of Pumping Test Data. International Institute for Land Reclamation and Improvement/ILRI. Wageningen, The Netherlands.

- Living Atlas, 2020, A-10 m Resolution map of earth's ;andsurface from 2020, developed by Impact Observatory. https://livingatlas.arcgis.com/landcover/ Accessed on 19th January 2023.

- Logan, J., 1964, Estimating transmissivity from routine production tests of water wells. Groundwater, 2(1): 35-37. https://doi.org/10.1111/j.1745-6584.1964.tb01744.x

- Mandel, S., Shiftan, Z.L., 1981, Groundwater Resources – Investigation and Development, Academic Press, Inc., New York

- Mazac, O., Kelly, W.E., Landa, I., 1985, A hydrogeophysical model for relations between electrical and hydraulic properties of aquifers. Journal of Hydrology. 79, 1-19.

- Meijerink, A.M.J., 2007, Remote sensing applications to groundwater. Paris: United Nations Educational Scientific and Cultural Organization (UNESCO).

- Minaibim, E.A., Iyeneomie, T., Opiriyabo, Ibim I.H., 2022, Aquifer Delineation using Seismic Refraction Method in Rumuohia Community, Emohua L.GA, Rivers State, Nigeria, Earth Sciences Pakistan, 6(1): 17-21.

- Nigeria Geological Survey Agency (NGSA), 2006, Published by the Authority of the Federal Republic of Nigeria.

- Nwosu, L.I., Ekine, A.S., Nwankwo, C.N., 2013, Evaluation of Groundwater Potential from Pumping Test Analysis and Vertical Electrical Sounding Results: Case Study of Okigwe District of Imo State Nigeria. The Pacific Journal of Science and Technology, Volume 14. Number 1, 536 – 548. http://www.akamaiuniversity.us/PJST.htm

- Obaje, N.G., 2009, Geology and Mineral Resources of Nigeria. Springer- Verlag, Berlin, 218p.

- Olasehinde, P.I., Amadi, A.N., Idris-Nda, A., Katu, M.J., Unuevho, C.I., Jimoh, M.O., 2015, Aquifers Characterization in Agaie, North-Central Nigeria Using Electrical Resistivity Method and Borehole Lithologs. American Journal of Environmental Protection, 2015, Vol. 3, No. 3, 60-66. Available online at http://pubs.sciepub.com/env/3/3/1

- Omer, AM., 2018, Sustainability Criteria for Water Resource Systems: Sustainable Development and Management. Int. J. Adv Res Water Resc Hydr Engi 2018; 1(1&2): 1-19.

- Opeyemi, J., Akinrinade, A., Rasheed, B., Adesina, A., 2016, Hydrogeophysical investigation of groundwater potential and aquifer vulnerability prediction in basement complex terrain – A case study from Akure, Southwestern Nigeria. RMZ – M&G 2016, Vol. 63, pp. 55–066, DOI:10.1515/rmzmag-2016-0005

- Poehls, D.J., Smith, G.J., 2009, Encyclopedic Dictionary of Hydrogeology. Elsevier Academic Research Incorporation, Amsterdam, ISBN 978-0-12-558690-0, p. 518.

- Raghunath, H.M., 1987, Groundwater. Wiley Eastern Ltd., Delhi.

- Saaty, I.T., 2006, Rank from comparisons and from ratings in the analytical/network processes. European Journal of operational Research, Vol. 168, pp. 557-570.

- Saaty, I.T., 1990, How to make a decision: the analytic hierarchy process

- Saaty, I.T., 1980, The analytical hierarchy process, New York, McGraw-Hill International.

- Sajeena, S., Abdul Hakkim, V.M., Kurien, E.K., 2014, Identification of Groundwater Prospective Zones using Geoelectrical and Electromagnetic Surveys. International Journal of Engineering Inventions, 3(6), pp. 17–21.

- Schwartz, F.W., Zhang, H., 2003, Fundamentals of Ground Water. Wiley, New York.

- Shaban, A., Khawlie, M., Abdalla, C., 2006, Use of GIS and remote sensing to determine recharge potential zones; the case of occidental Linanon. Hydrogeology Journal, 14(4), pp. 433–443.

- Subba Rao, N., 2017, Hydrogeology, problems with solutions. PHI Learning Private Limited, Delhi. Pp. 265.

- Tartiyus, E.H., Mohammed, I.D., Amade, P., 2015, Impact of population growth on economic growth in Nigeria (1980–2010). Journal of Humanities and Social Science (IOSR-JHSS), 20(4), 115–123. DOI: 10.9790/0837-2045115123.

- Tizro, T.A., Voudouris, K.S., Kamali, M., 2014, Comparative study of step drawdown and constant discharge tests to determine the aquifer Transmissivity: The Kangavar aquifer case study, Iran. J. Water Resource Hydraulic Eng., 3: 12-21.

- Todd, D.K., 1980, Groundwater Hydrology. 2nd edition, John Wiley, New York, 535 pp.

- Tsepav, M.T., Ibrahim, S.I., Bayegun, F.A., 2015, Geoelectrical Characterization of Aquifer Precincts in Parts of Lapai, North Central Nigeria. Journal of Applied Science and Environmental Management, 19(2), pp. 295– 301.

- Tweed, S.O., Leblanc, M., Webb, J.A., Lubczynski, M.W., 2007, Remote sensing and GIS for mapping groundwater recharge and discharge areas in salinity prone catchments, southeastern Australia. Hydrogeology Journal, 15(1), pp. 75–96.

- Utom, A.U., Odoh, B.I., Okoro, A.U., 2012, Estimation of aquifer Transmissivity using Dar Zarrouk parameters derived from surface resistivity measurements: A case history from parts of Enugu town (Nigeria). J. Water Resource Protect., 4: 993-1000. DOI: 10.4236/jwarp.2012.412115

- Vargas, L.G., 1990, An overview of the analytical hierarchy process and its applications. European Journal of Operational Research, 48: 2-8.

- Walton, W.C., 1991, Principles of Groundwater Engineering. Lewis Publishers, Inc., Chelsea, MI.

- Wilson, L.G., 1983, Monitoring in the vadose zone: Part 3. Groundwater Monitoring Review, 1983, 3(1), 155-166.